ISTANBUL TECHNICAL UNIVERSITY ★ GRADUATE SCHOOL OF SCIENCE ENGINEERING AND TECHNOLOGY

CLICK REACTION IN THE PRESENCE OF ACETIC ACID: A DFT STUDY

M.Sc. THESIS

Gamze KARAGAÇTI

Department of Chemistry

Chemistry Programme

JUNE 2014

ISTANBUL TECHNICAL UNIVERSITY ★ GRADUATE SCHOOL OF SCIENCE ENGINEERING AND TECHNOLOGY

CLICK REACTION IN THE PRESENCE OF ACETIC ACID: A DFT STUDY

M.Sc. THESIS

Gamze KARAGAÇTI
(509101060)

Department of Chemistry

Chemistry Programme

Thesis Advisor: Assoc. Prof. Dr. Nurcan TÜZÜN

JUNE 2014

İSTANBUL TEKNİK ÜNİVERSİTESİ ★ FEN BİLİMLERİ ENSTİTÜSÜ

ASETİK ASİT VARLIĞINDA GERÇEKLEŞEN KLİK REAKSİYONLARI: BİR DFT ÇALIŞMASI

YÜKSEK LİSANS TEZİ

Gamze KARAGAÇTI
(509101060)

Kimya Anabilim Dalı

Kimya Programı

Tez Danışmanı: Doç. Dr. Nurcan TÜZÜN

HAZİRAN 2014

Gamze Karagaçtı, a **M.Sc.** student of ITU **Graduate School of Science Engineering and Technology.** student ID 509101060, successfully defended the **thesis** entitled "**CLICK REACTION IN THE PRESENCE OF ACETIC ACID: A DFT STUDY** ", which she prepared after fulfilling the requirements specified in the associated legislations, before the jury whose signatures are below.

Thesis Advisor : **Assoc. Prof. Dr. Nurcan TUZUN**
İstanbul Technical University

Jury Members : **Prof. Dr. Mine YURTSEVER**
İstanbul Technical University

Assoc. Prof. Dr. Fethiye Aylin SUNGUR KONUKLAR
İstanbul Technical University

FOREWORD

I wish to express my appreciation to Assoc. Prof. Dr. Nurcan TÜZÜN, for supporting and giving advice to me since the beginning of this thesis.

I would like thank our group members Esra Boz and Cihan Özen for their all kind of asssistances.

My special thanks to my family and all of my friends, who give their support and love in my whole life. My boyfriend, Görkem Akagündüz, also deserves very special thanks for his patience, understanding and being my side during the months it took to complete my study.

May 2014

Gamze KARAGAÇTI
Chemist

TABLE OF CONTENTS

Page

ABBREVIATIONS

B3LYP	**:** Becke Style Three Parameter Functional in Combination with the Lee-Yang Parr Correlation Functional
DFT	**:** Density Functional Theory
E	**:** Energy
G03	**:** Gaussian 03
H	**:** Hamiltonian Operator
HF	**:** Hartree-Fock
IRC	**:** Intrinsic Reaction Coordinate
LDA	**:** Local Density Approximation
CuAAC	**:** Copper-Catalyzed Azide-Alkyne Cycloaddition

LIST OF TABLES

Page

LIST OF FIGURES

Page

CLICK REACTION IN THE PRESENCE OF ACETIC ACID: A DFT STUDY

SUMMARY

The developing chemical synthesis methods make significant contributions to industry and science. Metal catalysts have many advantages such as: shortening the reaction times, increasing efficiency of reactions, being able to design tailor-made products and performing environmentally friendly processes. In this respect, metal-catalyzed reactions are considered as one of the most important leading subjects in the field of modern chemical synthesis.

Copper-catalyzed azide-alkyne cycloaddition reaction (CuAAC), which was developed by Fokin, Sharpless and their teams in 2002, gained its place in the literature as a major breakthrough in modern chemical synthesis methods. In this 'click chemistry', a terminal alkyne forms 1,2,3-triazole derivatives in the presence of copper catalyst. This method has been the subject of numerous studies and gained its place in many fields of industry since it takes place at lower temperatures, with a high product yield in a regioselectivite way.

In this thesis, the protonation and cycloaddition steps of copper-catalyzed azide-alkyne cycloaddition reaction, a synthesis method of 1,2,3 triazole derivatives used in many fields of industry, have been studied and elaborated. In recent studies, acetic acid was reported to decrease the reaction times dramatically. In this thesis study, the effect of acetic acid on both the cycloaddition and protonation steps of CuAAC reaction mechanism has been modelled by quantum mechanical calculations. As for the methodology, for copper and nitrogen atoms B3LYP/6-31+G* and for the rest B3LYP/6-31G* basis sets have been used. In the presence of acetic acid, it can act as ligand. In modelling, initial copper-acetylide structure containing one acetate group as ligand has been considered. The cycloaddition starting with this structure has not shown a significant decrease in the barriers as compared to the case with no acetic acid as ligand.

In this study, the protonation step which is the final part of the reaction has been modelled for two different cases where the acetic acid or the alkyne act as H donors. In the presence of acetic acid, with both ligand and donor, the reaction is much more facile as compared to the case where alkyne is the H-donor. In the absence of acetic acid as ligand, protonation is again much more facile with acetic acid as H-donor as compared to the alkyne. The energy values indicate that in the reaction medium, acetic acid will be the proton donor, which is also in accordance with basic chemical knowledge. More important data is the comparison of protonation paths starting from copper-triazolide structure with or without acetate group as ligand, where acetic acid is the proton donor. Among all the possibilities, the lowest barrier was observed for the case where acetic acid is acting both as ligand and as H-donor. Thus, it can be concluded that acetic acid is facilitating the reaction not only as an easy proton donor, but also acting as ligand and accelerating the reaction.

Cycloaddition reaction in the presence of acetate as ligand decreases the barrier by approximately 2 kcal/mol. Without acetate ligand, considering the overal reaction, H

abstraction step is highly energy requiring and can be the rate determining step of the reaction. However, in the presence of acetate both as ligand and donor, protonation is facile and cannot be rate determining step. Depending on the reaction conditions, protonation could be faster or slower. Similar results were reported in the literature where facilitating an acidic environment has decreased the reaction times to a great extent. In this respect, our results show that protonation step has a crucial role on the kinetics of the CuAAC reactions and they are in accordance with the experiments.

Although the early studies have indicated that the CuAAC mechanism works through a single copper, several studies performed afterwards suggested that the reaction rate constant was second order with respect to copper. In recent years, it has been reported in a great number of experimental and theoretical publications in literature that the CuAAC reactions worked through multi-nuclear copper complexes. Özen et al have performed DFT calculations on a number of copper-alkyne complexes including mono to four copper centers and have concluded that 4-centered copper-complex is more prone to be formed, based on thermodynamic data. Two-copper centered complexes have not been excluded since both structures have revealed almost the same barrier for cycloaddition step of the click reaction.
On the other hand, upon the experimental demonstration in a current release on the number of copper metals involved in copper complexes in CuAAC reactions a mechanism involving ligand has been suggested to take place via two copper atoms. In this study, isotopic labelling on Cu atoms has been utilized. Based on the suggested structures from the mentioned study, dissertation study was broadened and the recent experimental publication has been taken as reference. The two-copper species from this study were modelled as a part of this thesis. The energies of various copper acetylide structures, created according to the experimental publication was modelled by considering the structures at two different level of studies.

ASETİK ASİT VARLIĞINDA GERÇEKLEŞEN KLİK REAKSİYONLARI: BİR DFT ÇALIŞMASI

ÖZET

Her geçen gün gelişen kimyasal sentez yöntemleri endüstri ve bilime katkıları da beraberinde getirmektedir. Metal katalizörlerin kimyasal sentezde bir çok avantajları vardır. Bunlar, tepkime sürelerini kısaltabilmeleri, istenilen ürüne yönelik sentezi olası kılmaları ve çevre dostu proseslerin gerçekleştirilebilmesi olarak sayılabilir. Bu bağlamda metal katalizörler modern kimyasal sentez alanının en önemli konularının başında gelmektedir.

20. yy'ın ortalarında geliştirilen Huisgen Reaksiyon'unda azit ve alkin tepkimeye girerek triazol türevlerini meydana getirmektedir. Bu reaksiyonun seçiciliği olmadığı için tepkime sonunda 1,4 ve 1,5-disübstitüye triazol ürünlerinin bir karışımı elde edilebilmektedir.

2002 yılında Fokin, Sharpless ve ekipleri tarafından geliştirilen, bakır katalizörlü azit-alkin siklokatılma reaksiyonu (CuAAC), modern kimyasal sentez yöntemlerinde çok önemli bir gelişme olarak literatürde yerini almış ve bu tepkime klik tepkimesi olarak adlandırılmıştır. Klik kimyası yönteminde uç alkinden bakır katalizörlüğünde 1,2,3-triazol türevleri elde edilmektedir. Bu yöntem, düşük sıcaklıklarda gerçekleşmesi, yüksek ürün verimiyle sonlanması ve regioselektif olması sebebiyle bir çok çalışmaya konu olmuş ve endüstrinin birçok alanında kendine yer bulmuştur.

Reaksiyonun ilk adımında bakır atomu alkin molekülünün π elektronlarına koordine olup, üçlü bağın asitliğinden faydalanarak hızlıca deprotone olur ve bakır asetiliti meydana getirir. Daha sonraki aşamada azitteki nitrojen bakır ile van der Waals yapısı oluşturur. Bu aşamadan sonra azit grubunun uç nitrojeni karbona yaklaşarak 6'lı bir halka yapısını oluşturur. Reaksiyonun son aşamasında bakır-triazolit yapısı protonasyona uğrayarak triazol ürününü meydana getirir.

Bu tezde endüstrinin birçok alanında kullanılan 1,2,3-triazol türevlerinin sentez yöntemi olan bakır katalizörlüğünde gerçekleşen azit-alkin siklokatılma tepkimelerinin protonasyon ve siklokatılma basamakları çalışılmış ve detaylandırılmıştır.

Literatürde yer alan güncel bir çalışmada, CuAAC reaksiyon mekanizmasının son aşaması olan protonasyon basamağının zayıf bir asit varlığında, asitsiz ortama göre daha hızlı olacağı belirtilmiştir. Benzer sonuçlar yine bir başka çalışma grubu tarafından da, asidik bir ortamda gerçekleşen CuAAC reaksiyonu protonasyon aşamasının, reaksiyon hızında ciddi bir artış sağladığı ve reaksiyon zamanını kısalttığı şeklinde rapor edilmiştir. Ayrıca grubumuzda yapılan henüz yayınlanmamış bir çalışmada, protonasyon basamağı asetik asit varlığında modellenmiş ve yapılar arası geçiş bariyerlerinin asetik asitsiz protonasyona göre daha düşük olduğu saptanmıştır.

Bu tez kapsamında CuAAC reaksiyonunun protonasyon aşaması asetik asit varlığında modellenmiş, tepkime patikasında bulunan yapıların asetik asit varlığında ne tür yapısal ve termodinamik değişimler gösterdiği incelenmiştir. Ayrıca asetik asitin CuAAC reaksiyon mekanizmasının siklokatılma basamağını da

hızlandırabileceği düşünülmüştür. Bu yüzden asetik asit varlığında siklokatılma basamağının modellenmesi de tez kapsamına alınmıştır.
Tezin ilk bölümünde CuAAC tepkimesine asetik asidin etkisi 2 ayrı kısımda incelenmiştir.
1) Ligant olarak 1 asetat içeren bakır asetilit yapısı ile başlayan CuAAC tepkimesinin siklokatılma aşamasında enerji geçiş bariyerleri hesaplanmış ve elde edile veriler asetik asitin ligand olarak bulunmadığı siklokatılma mekanizması enerji geçiş bariyerleri ile kıyaslanması yapılmıştır
Çalışmaya ligant olarak 1 asetat bulunduran bakır asetilit yapılarının modellenmesi ile başlanmıştır. Bu aşamada ligant iki oksijenden ve tek oksijenden olmak üzere iki farklı şekilde bağlanabilmektedir. Her iki olasılık için mekanizmalar ayrı ayrı modellenmiş ve sonuçları birbirleriyle karşılaştırılmıştır.
En düşük enerjili, ligant olarak 1 asetat içeren bakır asetilit yapısından başlanarak siklokatılma mekanizması modellenmiş ve sonuçlar grubumuzda yapılan asetatsız çalışma ile kıyaslanmıştır. Çalışmanın siklokatılma aşamasında tepkimenin literatüre uygun olarak, azit nitrojeninin bakır ile van der Waals yapısı oluşturması ile başladığı gözlemlenmiştir. Bu aşamadan sonra uç nitrojen alkin karbonu ile 6 üyeli bakır-triazolit halkasını oluşturmuştur. Asetik asit varlığında siklokatılma basamağı enerji bariyeri, asetik asit bulunmayan siklokatılma reaksiyonuna göre yaklaşık 2 kcal/mol daha düşük bulunmuştur.
2) Ligant olarak bir asetat içeren bakır triazolit yapısı ile başlatılan CuAAC reaksiyonunun protonasyon basamağında,
a) Asetik asitin H donörü olduğu durumdaki enerji geçiş bariyerlerinin hesaplanması
b) Alkinin H donörü olduğu durumdaki enerji geçiş bariyerlerinin hesaplanması
ve sonuçların birbirleri ile ve önceki çalışmalarla karşılaştırılması amaçlanmıştır.
Reaksiyonun son kısmı olan protonasyon basamağı, asetik asitin H donörü olduğu ve alkinin H donörü olduğu iki farklı durum için modelleneceğinden 2 ayrı protonasyon model mekanizması oluşturulmuştur.
Elde edilen sonuçlar asetik asitin H donörü olduğu durumda, alkin ile gerçekleşen protonasyona göre daha düşük bariyerle gerçekleştiğini göstermiştir.
Veriler önceki çalışmalar ile kıyaslanmış ve asetatın ligant olarak var olduğu bakır triazolit yapısının, asetik asitle protonasyon bariyerlerinin asetatı ligand olarak bulundurmayan bakır triazolit yapısının asetik asitle protonasyon bariyerlerine göre anlamlı farklılıkların olmadığı tespit edilmiştir. Bu sonuçlara göre, asetik asit ile gerçekleşen protonasyon aşaması için bakır-triazolitte asetat bulunması yada bulunmamasının enerji bariyerlerinde herhangi bir değişiklik yapmayacağı söylenebilir.
Diğer taraftan da tezin ikinci bölümünde, CuAAC reaksiyonları için literatürde önerilmiş güncel reaksiyon mekanizması için modelleme yapılması amaçlanmıştır.
İlk çalışmalar CuAAC mekanizmasının tek bakır üzerinden yürüdüğünü belirtse de, sonrasında yapılan birçok çalışmada tepkimenin hız sabitinin bakıra göre 2. mertebeden olduğunu göstermiştir. Bu durumda çeşitli bakır-asetilit yapıları arasında dinamik bir denge olduğu söylenebilir.
Ancak son yıllarda literatürde deneysel ve teorik çok sayıda yayında, CuAAC reaksiyonlarının 4 bakır üzerinden yürüdüğü belirtilmiştir. Aynı zamanda grubumuz tarafından yapılan bir tez çalışmasında CuAAC mekanizması 2,3 ve 4 bakırlı olarak modellenmiş ve sonuçlar literatürle uyumlu olarak 4 bakırlı asetilit yapılarının en düşük enerjili olduğu saptanmıştır.
Ancak konuyla ilgili literatürde yayınlanmış, güncel bir yayında bakır katalizörlü azit-alkin siklokatılma reaksiyonlarında mekanizmanın 2 bakır üzerinden

yürüdüğünün deneysel olarak gösterilmesi üzerine, tez çalışması genişletilmek istenmiş ve yapılan son deneysel yayın referans alınarak CuAAC reaksiyon mekanizması 2 bakır üzerinden modellenmek istenmiştir.

CuAAC reaksiyon mekanizmasını aydınlatmak amacıyla 2 farklı bakır izotopu kullanılarak yapılan ve tarafımızca referans alınan deneysel çalışmada, CuAAC reaksiyon mekanizmasının 2 bakır üzerinden yürüdüğü belirtilmiştir. Çalışmada N-heterosiklikkarben (NHC) bağlı, doğal izotopik orana sahip olan bakır içeren bakır asetilit yapısı, yalnızca bakır 63 izotopuna sahip Tetrakisbakır(I)asetonitrilhekzaflorofosfat varlığında benzilazit ile tepkimeye sokulmuştur. Reaksiyon sonunda izole edilen bakır triazolit yapısının analizi sonucunda ^{63}Cu : ^{65}Cu oranı 85:15 olarak bulunmuştur. Bu sonuçlara göre, reaksiyon sırasında bakırlar arası ligand değişiminin gerçekleştiği, izotop oranlarındaki değişmenin nedeninin NHC ve MeCN arası göç olduğu söylenmiştir.

Tüm bu bilgilerin ışığında tez çalışmasında CuAAC mekanizmasına farklı bir bakış getiren çalışmanın önerdiği mekanizmanın modellenmesi amaçlanmıştır.

Öncelikle önerilen mekanizmada yer alan izole edilmiş NHC bağlı bakır asetilit yapısı modellenmek istenmiştir. Bu yapı için çeşitli geometriler önerilmiş ve farklı DFT fonksiyonları ile denemeler yapılmıştır.

NHC bağlı bakır asetilit yapısı için olası 2 ana yapı tespit edilmiş ve bu yapıların kendi içlerinde nötral dublet ve +1 yüklü singlet yapıları ayrı ayrı modellenmeye çalışılmıştır.

Yapıların tespiti sırasında akla gelen ilk soru ana NHC bağlı bakır asetilit yapısı ile bağ yapacak olan bakırın kaç MeCN bulunduracağı idi. Bu anlamda, öncelikle, ligant olarak 1 MeCN taşıyan bakır ve NHC bağlı bakır asetilitin etkileşiminin modellenmesine karar verildi. Daha sonra bu yapının hem nötral dublet hem de +1 yüklü singlet versiyonları için ayrı ayrı modelleme yapıldı.

2. olası yapı olan, ligant olarak 2 MeCN taşıyan bakır ve NHC ligantlı bakır asetilitin etkileşimi de nötral dublet ve +1 yüklü singlet olarak ayrı ayrı modellendi.

Bu çalışmalar öncelikle B3LYP fonksiyonu kullanılarak yapıldı. Hesaplar sırasında karşılaşılan sorunlar nedeniyle, tüm olası yapılar, literatürde bakır için iyi sonuçlar verdiği öne sürülen M06L fonksiyonu ile tekrar modellenmeye çalışıldı.

1. INTRODUCTION

Developing chemical synthesis methods contributes to industry and science. Shortening the reaction times, performing environment-friendly processes and designing reactions with metal catalysts that give custom-made products with high efficiency are in this sense, considered as the most important leading subjects in the field of modern chemical synthesis.

In this thesis, the protonation and cycloaddition mechanisms of copper-catalyzed azide- alkyne cycloaddition reaction, which is a synthetic method of 1,2,3-triazole derivatives used in many scientific disciplines [1-6], have been studied and elaborated.

Triazole family of compounds provides important advantages in chemical synthesis. Their chemical stabilities which do not change even at high temperatures cause them to remain inert under severe hydrolytic, oxidizing and reducing conditions. The fact that they are so significant in the field of chemical synthesis is due to their unique position and various biological activities in heterocyclic chemistry. In this way, triazole products can be applied in many fields of treatment. Thus, they operate in several units of the pharmaceutical field, such as the treatment of fungal infections [7-10], HIV[11], allergy [12] and various microbial diseases [13-15]. The conducted researches have suggested that triazoles have also been effective on cancer known as the disease of our age. Today many triazole derivatives play an efficient role in the treatment of liver [16], breast [17], prostate and pancreatic cancers [18]. In addition to all of these, the anti-inflammatory [19-21], antidepressant [22] and analgesic activities [21] of the triazole derivatives broaden their field of application and increase their significance in the medical field.

The Huisgen Reaction developed in mid-20th century produced the triazole derivatives via thermal reaction of an azide and an alkyne. Huisgen reaction had basically several disadvantages. The fact that a high temperature was required for the reaction made it difficult to control the reaction, and the low reaction rate and efficiency restricted the field of application of the reaction [23-28]. Since the differences in HOMO-LUMO energy levels for both azides and alkynes are of

similar magnitude, both dipole-HOMO and dipole-LUMO controlled pathways operate in these cycloadditions [29]. As a result, the disubstituted triazole products-1,4 and 1,5, were also formed at the end of the reaction [30-31].

In this sense, the copper-catalyzed azide-alkyne cycloaddition reaction (CuAAC), which was developed by Meldal, Sharpless and their teams in 2002, gained its place in the literature as a major break through in modern chemical synthesis methods. In this "click chemistry", a terminal alkyne forms the triazole derivative 1,2,3- in the presence of a copper catalyst [32].

The CuAAC reaction designed and put into practice by Sharpless and Meldal's team almost completely eliminated the disadvantages of Huisgen reaction. Since the activation barriers of the catalytic reaction is rather low compared to then non-catalytic reaction, the CuAAC reaction occurs 10^7 times faster than Huisgen. CuAAC reaction ending with high efficiency even at low temperatures makes it possible to obtain the desired triazole derivatives without any emerging by-product [33]. In CuAAC reaction, the steric and electronic properties related to the azide and alkyne centers do not affect the progress of the reaction to a considerable extent, therefore, the reaction runs smoothly in many protic and aprotic solvents, including water [34]. Variously substituted terminal alkynes generally react well with several types of azides including primary, secondary, tertiary, electron-defficient and electron-rich, aliphatic, aromatic and heteroaromatic azides [35].

In the proposed CuAAC reaction mechanism (Figure 1.1), at the first step of the reaction, π electrons of the alkyne molecule are coordinated with copper and rapidly get deprotonated by making use of the acidity of the triplebond (Step (A) in Figure 1.1) and form the copperacetylide. In the next stage, the nitrogen in azide forms a Van der Waals structure with copper (Step (B) in Figure 1.1). Following this stage, the terminal nitrogen of the azide group approaches carbon and forms a 6-membered structure (Step (C) in Figure 1.1). In the final stage of the reaction, the copper-triazolide structure undergoes protonation(Step (E) in Figure 1.1) and generates the triazole product.[35-40]

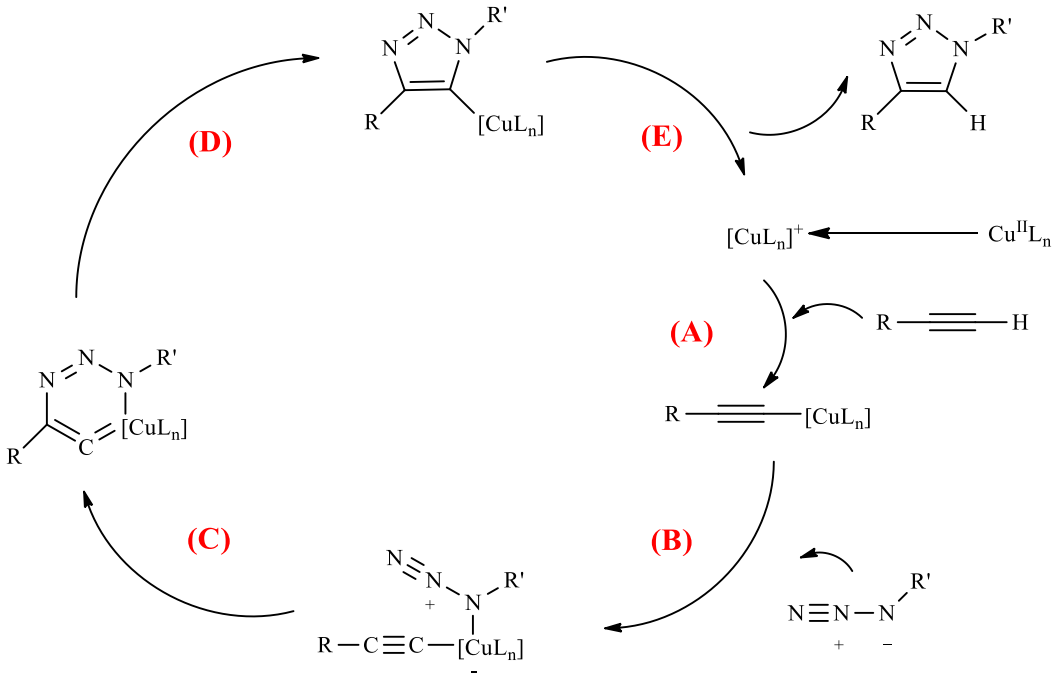

Figure 1.1: General route for a CuAAC reaction.

Most of the studies on CuAAC mechanism, carried out to date, have been concerned with the cycloaddition stage of the mechanism [34-43]. The studies regarding the final stage of the mechanism which is the protonation stage at which triazole is separated from the structure are rather limited.

In the literature, it was pointed out by Straub et.al. [44] that the protonation step, which is the final stage of CuAAC reaction mechanism, would be faster in the presence of weak acid. Similar results were also reported by Hu, et. al.expressing that the protonation stage of CuAAC reaction taking place in an acidic environment enabled a serious increase in the reaction rate and shortened the reaction period [45-46].

Separately, in a previous unpublished study performed in our group, the protonation stage of CUAAC reaction was modelled in the presence of acetic acid, during which the acetic acid was reported to have increased the reaction rate.

In accordance with all the developments, it was considered that the acetic acid would also affect the cycloaddition stage of CUAAC reaction mechanism. Thus, modeling the cycloaddition stage in the presence of acetic acid was also included in the scope of the dissertation.

Hence, the first section of the dissertation was analyzed under two main headings as cycloaddition and protonation.

The cycloaddition stage of the CuAAC mechanism was started with a copperacetylide containing one acetate as the ligand, coming from the acetic acid. During the study, the energy barriers among all the transition states and intermediates of the cycloaddition stage were calculated and compared with the previous study released by our group. The mechanism at the protonation stage, which is the second part of the CuAAC mechanisms, was modelled in two separate ways as :

1) The protonation of the coppertriazole containing one acetate as the ligand, which takes place when acetic acid becomes the H- donor.
2) The protonation of the coppertriazole containing 1 acetate as the ligand, which takes place when the reactant alkyne becomes the H- donor.

The energy barriers for both of the conditions were calculated separately. The obtained results were compared with each other and with previous study in which the protonation with acetic acid in the absence of acetate as ligand.

In the second part of the study, the CuAAC reaction has been taken into account again but from a different perspective. To date, the CuAAC reaction mechanism has been the subject of numerous studies due to the significance of this reaction. The early studies performed indicated that CuAAC reaction mechanism takes place via one-copper metal in the copper-acetylide structure. The kinetic studies carried out in recent years have suggested that the CuAAC reaction mechanism is 2^{nd} order with respect to copper and the reaction has multinuclear nature within the mechanism. In addition to known data, the fact that the CuAAC reaction mechanism has multinuclear nature has been supported in a great number of theoretical and experimental studies. Also in a dissertation study, the starting copper-acetylide complex in CuAAC mechanism was modelled with 2, 3 and 4- coppers. In that study, 4-copper acetylide structures were proposed to form in the absence of ligands, based on their thermodynamic preferences and the tendency of copper to form polymeric copper-alkynes [43], results being in concordance with the literature. Two-copper structures revealing the same reaction barrier as four-membered path has indicated that the reaction can possibly take place via 2-copper centered species. In a later study by Fokin *et al.*, an experimental study on CuAAC has been conducted [47]. In their study, 2 different copper isotopes have been used in order to illuminate the

CuAAC reaction mechanism. From their work, they have suggested a mechanism functioning by means of two copper centers which have actively participated in the reaction.

In this dissertation study, the copper-acetylide complexes as suggested by Fokin et al have been modelled as a part of the CuAAC mechanism. In the mechanism suggested by Fokin et al, a two-centered copper-acetylide structure formed in the course of the reaction where a very steric ligand, N-heterocyclic ligand was used. In their study, they have started with a copper-acetylide where the copper had the natural distribution of copper isotopes. As copper-catalyst, only one isotope, ^{63}Cu, was added into the reaction mixture in the form of $^{63}Cu(MeCN)_4PF_6$ and an isotopically rich product was obtained. This implied that the two copper atoms actively participated in the reaction. Accordingly, they have proposed copper-acetylide structures that formed at the beginning of the reaction. As a part of this thesis, these copper-acetylide structures are modeled. The second part of this thesis attempts to find the extent of the accuracy of the proposed copper-acetylide structures.

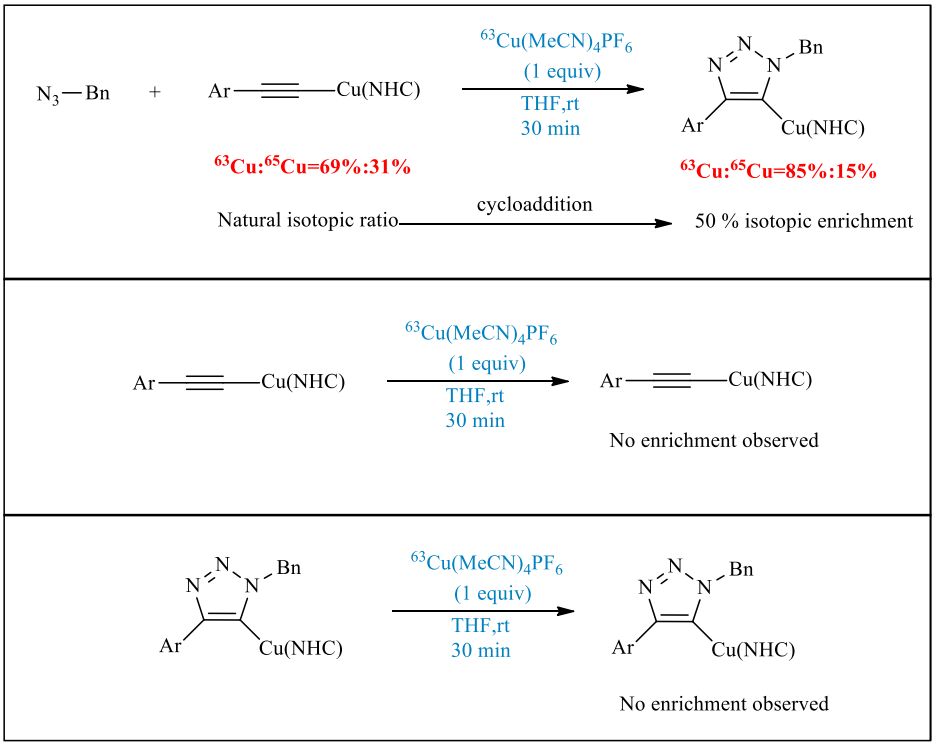

Figure 1.2 : Isotope enrichment experiments reported by Fokin *et al*. [47].

2. THEORY

The electronic structure methods use the principles of quantum mechanics. The energy and other related properties of a system may be obtained by solving the Schrödinger equation for this system:

$$\mathbf{H}\Psi = E\Psi \qquad \textbf{(2.1)}$$

where, Ψ is a wavefunction describing the x, y and z spatial coordinates of the particles in the system, E means the energy of the system at that state and **H** is the Hamiltonian operator for kinetic and potential energy of a system. The exact solution of Schrödinger equation is impossible for structures having more than single electron. Hence, some approximations are used in electronic structure methods. The mostly encountered three major classes of electronic structure methods are:

- Semi-empirical methods are based on the Hartree–Fock formalism, but make many approximations and obtain some parameters from empirical data.
- Ab initio methods, no experimental parameters are used.
- Density functional methods, the total energy of the system only depends on the electron density.

2.1 Semi-empirical Theory and Ab-initio Methods

In ab initio method, the Hamiltonian and the wavefunction (Ψ) have been defined, by use of the variational method,which enables calculation of electronic energy. In the variational method, the best wavefunction is found by minimizing the effective electronic energy with respect to parameters in the wavefunctions.

The accuracy of this method depends on the chosen wavefunction. However, for large molecules and complex wavefunctions, ab-initio calculations become computationally more expensive [48].

The difficulty of ab-initio calculations on large molecules led to development of semi-empirical methods. In semi-empirical methods, rather than solving all the integrals of the Schrödinger equation, parameters originating from experimental data

are used. Semi-empirical models can be used to yield continuous energy surfaces. They are neither variational nor size consistent. More importantly, semi-empirical methods are inherently dependent on the choice of parameters. The parameterization is tested against a limited set of molecules to ensure its accuracy. This dependence on parameters can be minimized by using a large and varied training set of molecules to establish parameters. This process is a continuing one. Parameters are introduced in order to reproduce experimental equilibrium geometries, heats of formation, electric dipole moments and ionization potentials.

2.2 Density Functional Theory

Density Functional Theory (DFT) is a theory in which ground state energy is expressed in terms of electron density [49-52]. This method was proposed by P. Hohenberg and W. Kohn in 1964 but it contained only virtual functionals. In 1965, Kohn and Sham brought formal functionals based on total electron density. Contrary to Hartree-Fock method [53-55], DFT has smaller computational cost with high accuracy. Although both methods account for the instantaneous interactions of pairs of electrons with opposite spin, DFT methods include the effects of electron correlation (electrons in a molecular system react to one another's motion and attempt to keep out of another's way) while Hartree-Fock calculations see this effect in an average sense (each electron sees and reacts to an averaged electron density).

Density functional methods partition the electronic energy into several terms and compute them separately.

$$E = E_T + E_V + E_J + E_{XC} \qquad \textbf{(2.2)}$$

E_T is the kinetic energy term, E_V is the potential energy of the nuclear-electron attraction and nuclear-nuclear repulsion term, E_J is the electron-electron repulsion term (also called Coulomb energy), E_{XC} is the exchange-correlation term that includes the remaining part of the electron-electron interactions and it is not known how to calculate exactly.

All the terms except the nuclear-nuclear repulsion, are functions of electron density, $\rho(r)$. E_{XC} can be categorized into exchange and correlation functionals. E_{XC} accounts for the exchange energy arising from the antisymmetry of the quantum mechanical wavefunction and the dynamic correlation in the motions of the individual electrons.

The variational principle determines the ground state energy and electron density in terms of the electron density. Further, the ground state electron density $\rho(r)$ determines the external potential, $v(r)$ and variationally determines the ground state properties of the system of interest.

The electronic energy can be expressed as a functional of the electron density:

$$E[\rho]=\int v(r)\rho(r)dr + T[\rho] + V_{ee}[\rho] \quad \textbf{(2.3)}$$

where $T[\rho]$ is the kinetic energy of interacting electrons and $V_{ee}[\rho]$ is the interelectronic interactions.

The electronic energy may be written in the form of Kohn-Sham approach.

$$E[\rho]=\int v(r)\rho(r)dr + T_s[\rho] + J[\rho] + E_{xc}[\rho] \quad \textbf{(2.4)}$$

This is based upon an orbital density description that removes the necessity of knowing the exact form of $T[\rho]$. Kohn-Sham proposed focusing on the kinetic energy of non-interacting system of electrons $T_s[\rho]$, as a functional of a set of single particle orbitals that give exact density.

$$T_S[\rho] = \sum_{i=1}^{N} < \Psi_i \left| -\frac{1}{2}\nabla^2 \right| \Psi_i > \quad \textbf{(2.5)}$$

$J[\rho]$ represents the electron-electron repulsion (Coulomb energy), and $E_{xc}[\rho]$ is the exchange-correlation energy functional with its functional derivative called the exchange-correlation potential, $v_{xc}(r)$.

$$E_{xc}[\rho]= T[\rho]- T_s[\rho]+ V_{ee}[\rho]- J[\rho] \quad \textbf{(2.6)}$$

$$v_{xc}(r) = \frac{\partial E_{xc}[\rho]}{\partial \rho(r)} \quad \textbf{(2.7)}$$

$E_{xc}[\rho]$ is divided into two parts, namely an exchange functional, $E_x[\rho]$ and a correlation functional, $E_c[\rho]$.

$$E_{xc}[\rho] = E_x[\rho] + E_c[\rho] \quad \textbf{(2.8)}$$

$E_x[\rho]$ and $E_c[\rho]$ functionals can be both local and gradient-corrected functionals. Local or gradient-corrected functionals are called traditional functionals. Local functionals depend only on electron density ρ, while gradient-corrected fuctionals depend on both ρ and its gradient, $\Delta\rho$.

A system of non-interacting electrons moving in an external effective potential $v_{eff}(r)$ is shown as;

$$v_{eff}(r) = v(r) + \frac{\partial J[\rho]}{\partial \rho(r)} + \frac{\partial E_{xc}[\rho]}{\partial \rho(r)} = v(r) + \int \frac{\rho(r')}{|r - r'|} dr' + v_{xc}(r) \quad \textbf{(2.9)}$$

Now, an equation very similar to the Schrödinger Equation exists.

$$\left[-\frac{1}{2}\nabla^2 + v_{eff}(r) \right] \Psi_i = \varepsilon_i \Psi_i \quad \textbf{(2.10)}$$

(2.4), (2.5), (2.6), (2.7), (2.8), (2.9) are Kohn-Sham Equations.

In order to evaluate the exchange-correlation functional some approximations are made. The first one is the local density approximation (LDA). It is based upon a model of uniform electron gas. In the uniform electron gas model, a large number of electrons uniformly spread out in a cube where there is a uniform distribution of the positive charge to make the system neutral. It assumes that the charge density varies slowly throughout the molecule so that a localized region of the molecule behaves like a uniform electron gas The energy expression is:

$$E[\rho] = T_s[\rho] + \int \rho(r) v(r) dr + J[\rho] + E_{xc}[\rho] + E_b \quad \textbf{(2.11)}$$

where E_b is the electrostatic energy of the positive background. Since the positive charge density is the negative to the electron density, the equation reduces to:

$$E[\rho] = T_s[\rho] + E_{xc}[\rho] = T_s[\rho] + E_x[\rho] + E_c[\rho] \quad \textbf{(2.12)}$$

The exchange functional is given by:

$$E_x[\rho] = -C_x \int \rho(r)^{4/3} dr \quad \textbf{(2.13)}$$

C_x=0.7386, this form was developed to reproduce the exchange energy of a uniform electron gas.

DFT methods are defined by pairing an exchange functional with a correlation functional and can be named as traditional or hybrid functionals. Hybrid functionals include exact term in the exchange functional, whereas traditional functionals do not. BLYP (Becke's gradient-corrected exchange functional with Lee-Yang-Parr's gradient-corrected correlation functional) method is a traditional functional whereas, B3LYP (Becke style three parameter functional in combination with the Lee-Yang-Parr correlation functional) method [56], the linear combination of LDA, B88, exact and LYP functionals, is a hybrid functional:

$$E_{xc} = E_{xc}^{LDA} + a_0(E_x^{exact} - E_x^{LDA}) + a_x \Delta E_x^{B88} + a_c \Delta E_c^{non-local} \quad \textbf{(2.14)}$$

where ΔE_x^{B88} is the Becke's gradient correction, i.e. the second term at the right hand side of the equation (2.12) and the correction to the correlation ($\Delta E_c^{non-local}$) is provided by the Lee-Yang-Parr functional. But, LYP includes both local and non-local terms, then the correlation functional used is actually: $a_c E_c^{LYP} + (1 - a_c) E_c^{VWN}$ where E_c^{VWN} is the Vosko-Wilk-Nusair correlation energy. The parameters are specified by Becke by fitting the atomization energies, ionization potentials, proton affinities and first row atomic energies in the molecule set, a_0=0.20, a_x=0.72 and a_c=0.81. Hybrid functionals have proven to be superior to the traditional functionals.

2.2.1 Basis sets

A basis set is a serie of basis functions which is used to expressed molecular orbitals. The molecular orbitals are emphasized as a linear combination of basis funtions which are pre-defined one-electron atomic functions. The basis functions are categorized into two classes, Slater Type Orbitals (STO) and Gaussian Type Orbitals (GTO). Slater Type Orbitals have the functional form

$$\Theta_{abc}(x,y,z) = N x^a y^b z^c e^{-\zeta r} \quad \textbf{(2.15)}$$

N is the normalization constant, a, b and c are angular momentum (L= a+b+c). Gaussian type orbitals can be written as

$$\Theta_{abc}(x,y,z) = Nx^a y^b z^c e^{-\zeta r^2} \quad \textbf{(2.16)}$$

GTOs are preferable over STOs because of the computational efficiency although STOs are more accurate. Among the types of the basis sets (minimal basis sets, split valence basis sets, polarized basis sets, high angular momentum basis sets) the most popular one is the split valence basis set which is developed by Pople and his group termed as 3-21G, 4-31G, 6-31G. Split valence basis sets allow orbitals to change size but not the shape. Polarized basis sets remove this limitation by adding orbitals with angular momentum beyond the ground state configuration for each atom. In this study 6-31G*, also known as 6-31G(d) polarization basis set is used where d functions are added to heavy atoms [57].

2.2.2 Intrinsic reaction coordinate

Intrinsic Reaction Coordinate (IRC) [58-59] is a minimum energy reaction path on a potential energy surface in mass-weighted coordinates, connecting reactants to products via the transition state [60]. When a transition state is optimized with an imaginary frequency, it must be confirmed that it is the correct transition state by making IRC calculations. The IRC path is defined by the differential equation

$$\frac{d\mathbf{x}}{ds} = -\frac{\mathbf{g}}{|\mathbf{g}|} = \mathbf{v} \quad \textbf{(2.17)}$$

Where x is the mass-weighted coordinates, s is the path length and v is the negative normalized gradient [57].

2.2.3 Gdiis algorithm

The GDIIS method [61-63] is based on a linear interpolation (and extrapolation) of the available structures that minimizes the length of an error vector.

$$x^* = \sum c_i x_i \quad \text{where } \sum c_i = 1 \quad \textbf{(2.18)}$$

For each structure $\boldsymbol{x}_i$, an error vector is constructed using a quadratic approximation to the potential energy surface. Given an estimated Hessian, $\boldsymbol{H}$, a Newton–Raphson optimization step yields$\boldsymbol{x}_i^{SR}$.

$$x_i^{SR} = x_i + H^{-1} f_i \quad \textbf{(2.19)}$$

where $\boldsymbol{f}_i$ is the force (negative of the gradient) at $\boldsymbol{x}_i$. The error vector $\boldsymbol{e}_i$ is chosen as the displacement in this simple relaxation (SR) step:

$$e_i = x_i^{SR} - x_i = H^{-1} f_i \quad \textbf{(2.20)}$$

In the quadratic approximation, the error or *residuum* vector for $\boldsymbol{x}^*$ is the linear combination of the individual error vectors,

$$r = \sum c_i \, e_i = e^* \quad \textbf{(2.21)}$$

The coefficients c_i are obtained by minimizing $|\boldsymbol{r}|^2$ with the constraint $\sum c_i = 1$. This least-squares problem leads to the following set of equations:

$$\begin{pmatrix} a_{1.1} & \dots & a_{1.k} & 1 \\ \vdots & \ddots & \vdots & \vdots \\ a_{k.1} & \dots & a_{k.k} & 1 \\ 1 & \dots & 1 & 0 \end{pmatrix} \begin{pmatrix} c_1 \\ \vdots \\ c_k \\ \lambda \end{pmatrix} = \begin{pmatrix} 0 \\ \vdots \\ 0 \\ 1 \end{pmatrix} \quad \textbf{(2.22)}$$

where matrix $\boldsymbol{A}$ is defined as $a_{i,j} = \boldsymbol{e}_i^{\mathrm{T}} \boldsymbol{e}_j$ and λ is the Lagrangian multiplier arising from the previously mentioned constraint. These coefficients determine the intermediate point $\boldsymbol{x}^*$ that minimizes the length of the residuum vector. The residuum vector is equal to the simple relaxation step from $\boldsymbol{x}^*$, and the next point in the optimization is given by

$$x_{k+1} = x^* + r = \sum c_i \, (x_i + e_i) = \sum c_i \, x_i^{SR} \quad \textbf{(2.23)}$$

The new point can also be regarded as the same linear combination of the predicted geometries, $\boldsymbol{x}_i^{\mathrm{SR}}$, produced by simple relaxation from the earlier points [64].

3. METHODOLOGY

In the first part of the thesis, the DFT method employing the B3LYP functional [56] has been used to carry out the full optimization of the compounds of interest in the gas phase with the G09 package [65], where the cycloaddition and protonation mechanisms of CuAAC have been discussed in previous studies [39]. Regarding with time cost and accuracy, for copper and nitrogen atoms B3LYP/6-31+G* and for the rest B3LYP/6-31G* basis sets have been used. The stationary points were studied by vibrational frequency calculations. All transition states were confirmed to be saddle points by one imaginary frequency belonging to the reaction coordinate. The intrinsic reaction coordinate (IRC) was followed to validate the expected reactants and products for all transition state structures [58,59]. The energies discussed in the text are free energies at 298 K, unless otherwise stated. In the discussion, the following notation was used: The reaction can start from 4 different starting copper-acetylide structures. These are named with a prefix of **M1**. The **1** or **2** in **M1_1a** or **M1_2a** signifies the number of acetate ligands in the copper-acetylide structure. The proceding **a** or **b** denotes a specific binding of the group as presented in Figures 4.1 - 4.4. The intermediate and transition state structures obtained starting from a certain copper-acetylide structure (**M1_1a**, **M1_1b**, **M1_2a** or **M1_2b**) are named with the corresponding suffixes.

In the second part of the thesis, two different basis sets, B3LYP[66] and M06L [67] have been utilized at the 6-31+G* level where copper-complexes have been modelled. In this section, copper has been treated with LANL2DZ effective core potential. In the 3D structure of molecules, atoms have been shown with different colours of ball forms. For copper atoms brown, for nitrogen atoms blue, for oxygen atoms red and for all the rest of atoms grey balls have been used. In the 3D structure of thesis's second part, green balls designated the phenyl groups. All optimization calculations have been done with gdiis algorithm [61-63] as implemented in the G09 package .

Energy values shown in Figure 4.11 and Figure 4.22 have been calculated according to protonation path where the acetic acid is the H donor. In order to equalize the

number of atoms, in the calculations, energy value of acetic acid was added to cycloaddition path (Figure4.11). For equalizing the number of atoms in protonation mechanism where the alkyne is the H donor to the number of atoms in the protonation mechanism where the acetic acid is the H donor, energy values of acetic acid has been added to protonation and energy value of alkyne has been removed from path.

4. RESULTS AND DISCUSSION

4.1 The Effect of Acetic Acid on the Protonation and Cycloaddition Stages.

In this section of the dissertation, the main focus has been on the effect of acetic acid on the cycloaddition and protonation mechanisms in CuAAC reaction.

In the literature, it was pointed out by Straub.*et.al*. that the protonation step which is the final stage of CuAAC reaction mechanism would be faster in the presence of a weak acid [44]. Similar results were also reported by Hu *et.al*., expressing that the protonation stage of CuAAC reaction taking place in an acidic environment enabled a serious increase in the reaction rate and shortened the reaction time.[45,46] The protonation step could be the rate determining-step of the whole mechanism where an alkyne is the proton source. However, in the presence of acetic acid, cycloaddition step can also be effected by the ability of acetate to act as ligand in the system. Thus, to complement the whole picture in CuAAC reactions, modelling the cycloaddition and protonation stages in the presence of acetic acid was also considered as a part of the dissertation.

To enlighten the mechanism, cycloaddition and protonation steps were modelled at the following two stages in this study:

a) Cycloaddition : Modelling the cycloaddition step of CuAAC reaction, starting with a copper- acetylide structure containing 1 acetate as one of the ligands and comparison of the mechanism in terms of barriers and structures with the cycloaddition mechanism in the absence of acetic acid.
b) Protonation: Modelling the protonation stage of CuAAC reaction starting with the copper triazolide structure containing 1 acetate as one of its ligands for two different cases:
    i. Protonation with alkyne as H donor
    ii. Protonation with acetic acid as H donor

In a previous study, protonation step has been modelled with alkyne and acetic acid as H-donor in the absence of acetic acid that could act as ligand [68].In this study,

comparisons will be made between the previous data and the barriers obtained from the b section.

4.1.1 Cycloaddition

The study started by modelling the copper acetylide structures containing 1 acetate as a ligand. For the ligand to bind to the copper-complex, two possibilities are present: Asetate can bind to copper from one oxygen, or it can bind from two oxygens. Boths possibilities have been considered in modelling. In the copper-complex where one acetate, as ligand, took part in the structure via binding from 2 oxygens is designated as **M1_1a** (Figure 4.1) and the structure where binding is from one oxygen atom is shown as **M1_1b** (Figure 4.2). The comparison of the energies of **M1_a** and **M1_b** has shown that **M1_a** is 8.07 kcal/mol more stable than **M1_b**. Thus, the cycloaddition has been modelled, starting with **M1_a** structure. The different copper-acetylides with two acetate structures (**M1_2a,** Figure 4.3) and (**M1_2b,** Figure 4.4) and copperacetylide (Figure 4.5) were also modelled with the B3LYP functional and the results were compared with each other (Table 1.1).

When **M1_1a** and **M1_1b** structures are comparatively analyzed, it is seen that **M1_1b** has a planar geometry, whereas **M1_1a** has a geometry close to a boat form. In **M1_1a**, the bonding efficiency of oxygens to coppers are similar whereas in **M1_1b**, there is a 0.03 Å difference between the lengths of the two Cu-O bonds. The reduced efficiency of copper to make another bond or the repulsions between the non-bonding oxygen and copper may cause this slight difference.

When **M1_2a** and **M1_2b** structures are compared with each other, it is seen that **M1_2a** is 4.48 kcal/mol more stable than **M1_2b**. While **M1_2b** has a boat-like form due to the acetate structures opposite to each other, it has a symmetrical geometry. The geometry with the lowest energy among all the modelled copper-acetylide structures is **M1_2a**. Since the starting point of the thesis was determined as the copper acetylide containing one acetate as the ligand, **M1_1a** was selected as the initial conformation. The CuAAC mechanism that could be modelled with the **M1_2a** initial conformation has remained as a future work.

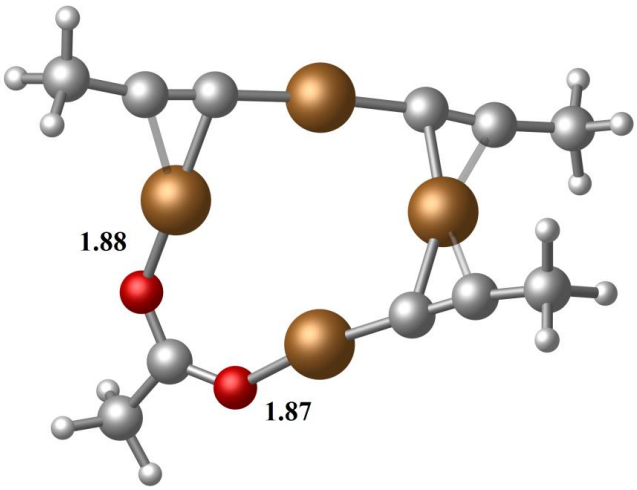

Figure 4.1 : The 3-dimensional structure of **M1_1a** structure.

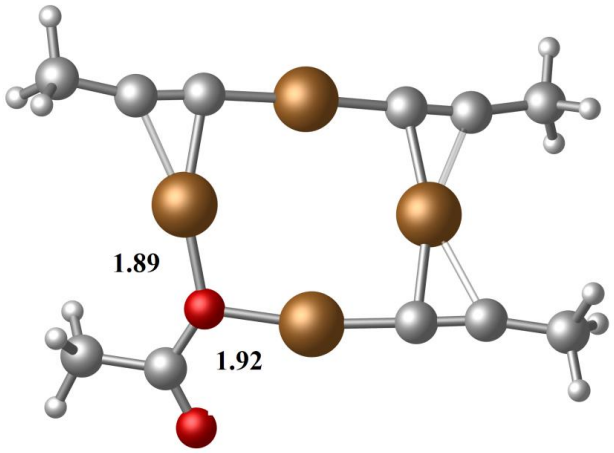

Figure 4.2 : The 3-dimensional structure of **M1_1b** structure.

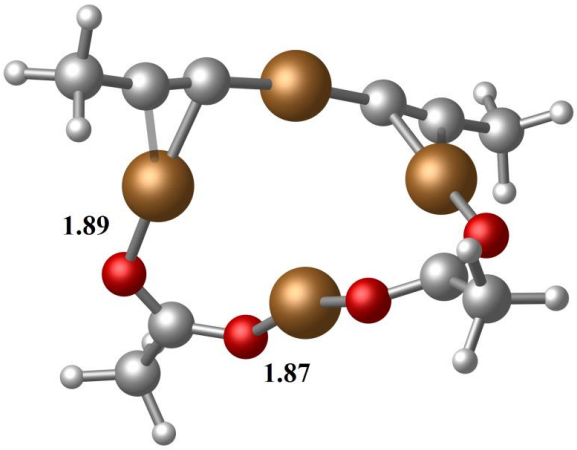

Figure 4.3 : The 3-dimensional structure of **M1_2a** structure.

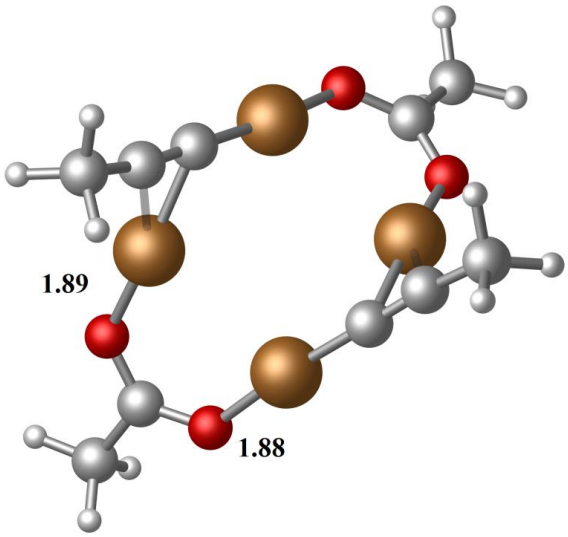

Figure 4.4 : The 3-dimensional structure of **M1_2b** structure.

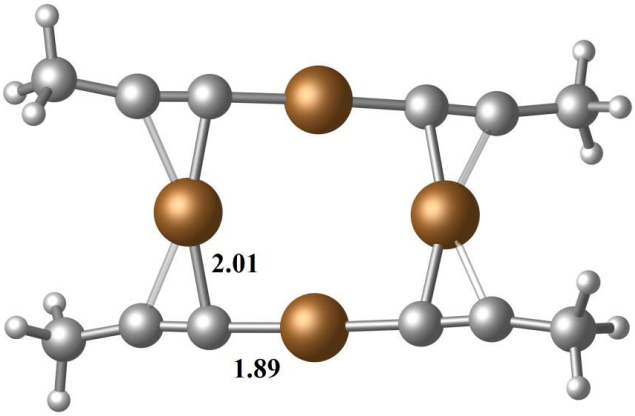

Figure 4.5 : The 3-dimensional structure of copper acetylide.

Table 4.1: Free Energies (in a.u.) and zero-point corrected electronic energies (E_{ZPE}) (in a.u.) of different copper acetylide structures containing one or two acetates as ligand.

Entry	***Free Energy***	***E_{ZPE}***
Propyn	-116.621777	-116.59755
Aceticacid	-229.037131	-229.010185
Copperacetylide	-7025.746412	-7025.686445
M1_a	-7138.186611	-7138.124112
M1_b	-7138.173741	-7138.11157
M1_2a	-7250.621336	-7250.557969
M1_2b	-7250.628482	-7250.565772

The cycloaddition mechanism was modelled by starting from the copper acetylide structure containing one acetate as the ligand with the lowest energy, and the results were compared with the previous studies performed in our group [10]. For the cycloaddition, the generally accepted mechanism that has been previously modelled by Ozen et al. has been considered. The reaction starts by the approaching azide group. A van der Waals complex is formed (**M2_1a**, Figure 4.6) at an expense of 7.6 kcal/mol from the starting copper acetylide structure. In this geometry, the azide and the Cu -C=C form a coplanar ring-like structure. The Cu-N binding distance is 2.28 Å. The Cu-C distances have slightly increased from 1.88 Å in **M1_1a** to 1.94 Å in **M2_1a** due to the loss of bonding of the reacting Cu with the alkyne. This structure could also be obtained from the preceeding transition state **M3_1a** (Figure 4.7).

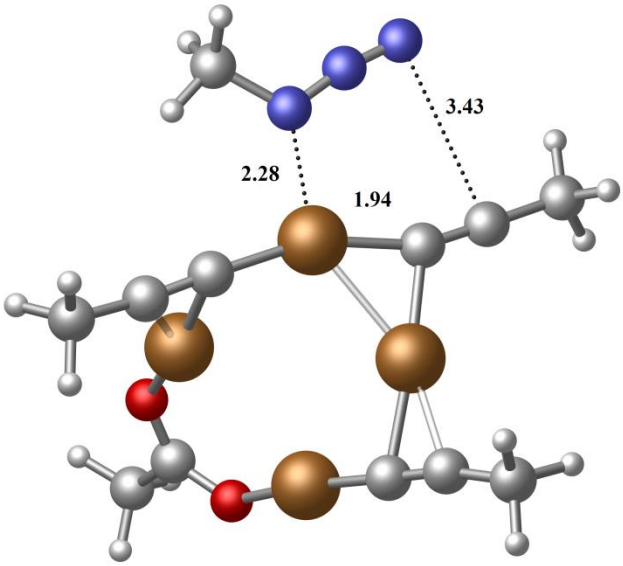

Figure 4.6 : The 3-dimensional structure of **M2_1a** structure.

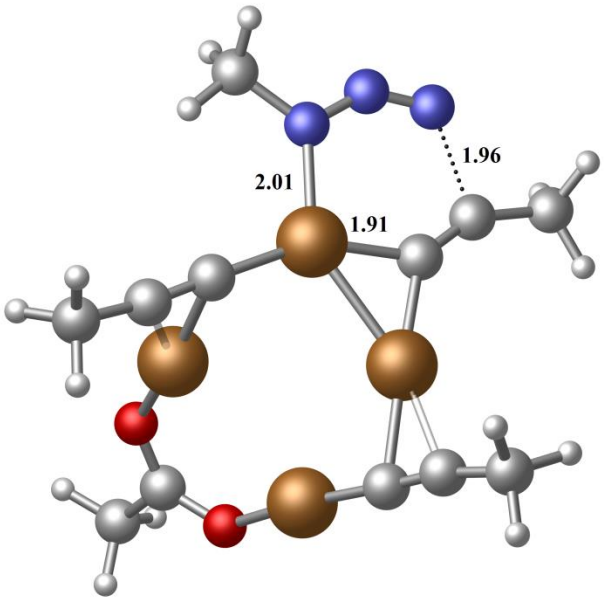

Figure 4.7 : The 3-dimensional structure of **M3_1a** structure.

By the approach of azide, binding from the terminal nitrogen takes place via **M3_1a** transition structure which leads to a 6-membered ring. In the course of the formation of the transition state, Cu-C=C fragment preserved its coplanar geometry and the approaching azide group has undergone a hybridization expecially in the internal

nitrogen to enable formation of the 6-membered ring in the same plane with Cu-C=C structure. The substituted olefinic carbon has also undergone hybridization in order to bind to terminal nitrogen. In **M3_1a** transition state, terminal nitrogen of the azide group is 1.96 Å away from the binding alkyne carbon and the other nitrogen of azide which will be bonding to Cu is 2.01 Å away from copper. From **M2_1a** to **M3_1a**, azide makes stronger bonding with the Cu-C=C fragment as expected and the bond lenghts changes according to this new bonding scheme.

In **M4_1a** structure a planar 6-membered ring forms by an efficient binding of terminal N and the terminal C in alkyne at 1.45 Å (Figure 4.8) distance. In **M4_1a** Cu and N has a stronger binding where the corresponding distance has decresed to 1.94 Å from 2.01 Å in **M3_1a** and 2.36 Å in **M2_1a**. Both alkyne carbons are sp^2 hybridized in accordance with the bonding pattern in the structure. The formation of the fused triazole ring has not caused a deformation in the main skeleton. For formation of triazole ring, the ring has to close for a 5-membered ring.

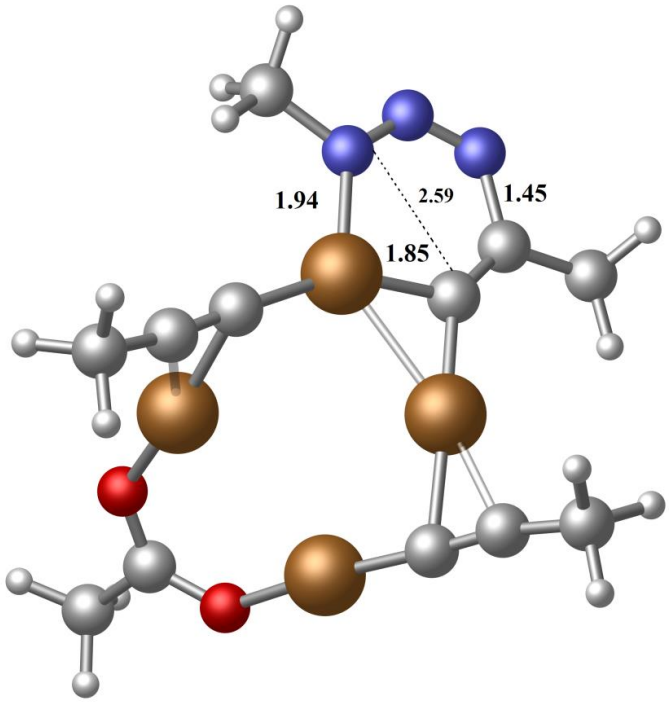

Figure 4.8 : The 3-dimensional structure of **M4_1a** structure.

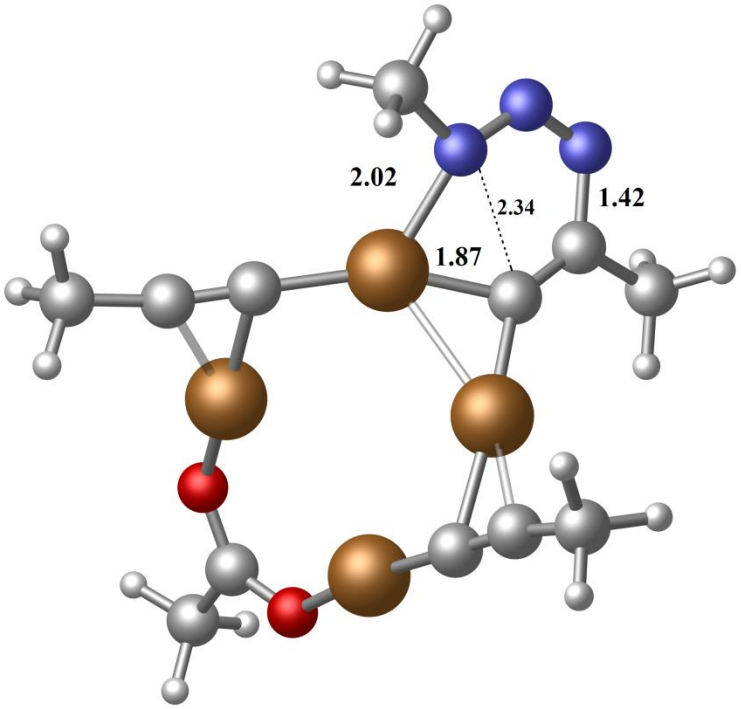

Figure 4.9 : The 3-dimensional structure of **M5_1a** structure.

After **M4_1a** intermediate, the bonding strength between Cu-N began to diminish (2.02 Å) to form a 5-membered triazole ring. In **M5_1a,** the distance of the nitrogen to the alkyne C that it will form a bond decreased to 2.34 Å which was 2.59Å in the **M4_1a** intermediate.

The alkyne π-bonding electrons which joined the azide resonance in the **M6_1a** intermediate facilitated the stabilization in this structure. The copper-triazolide ring forming as the last structure of cycloaddition mechanism will further undergo protonation to release the ring and to regenerate the catalyst (Figure 4.10).

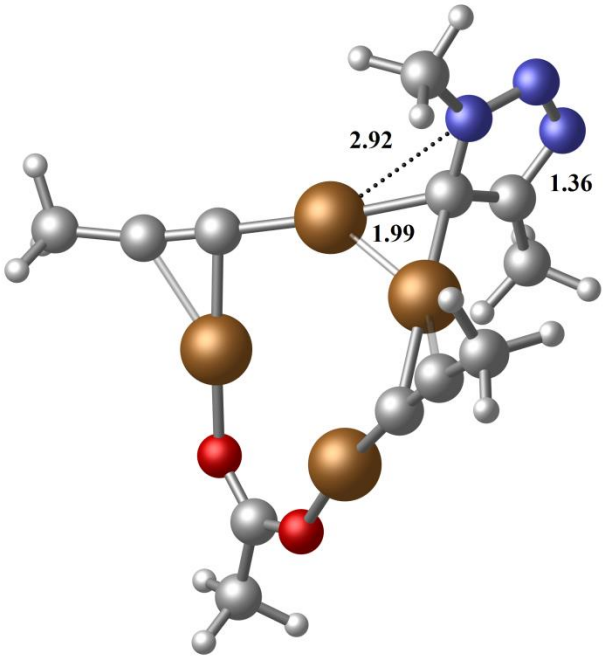

Figure 4.10 : The 3-dimensional structure of **M6_1a** structure.

The cycloaddition mechanism with acetate as ligand (Figure 4.11) is compared with the previous study (Figure 4.12). The transition states and the intermediates have similar geometries as compared to the path without the acetic acid such that the distances and angles at the active reaction center do not show extreme differences (**M3** and **M5**, from reference [68] in Figure 4.13 and Figure 4.14, respectively). In the absence of acetic acid, **M3** is the highest point on the path, where the analogous structure is again the highest structure in the case with acetic acid.

Comparison between the two paths shows that the **M2-M3/M2_1a-M3_1a** transition barrier was 2 kcal/mol lower in the path with the acetate as the ligand (Figure 4.11). The **M4-M5/M4_1a-M5_1a** transitions required the same energy barriers. This data implies that acetic acid acting as acetate ligand in the complex slightly facilitates the cycloaddition process.

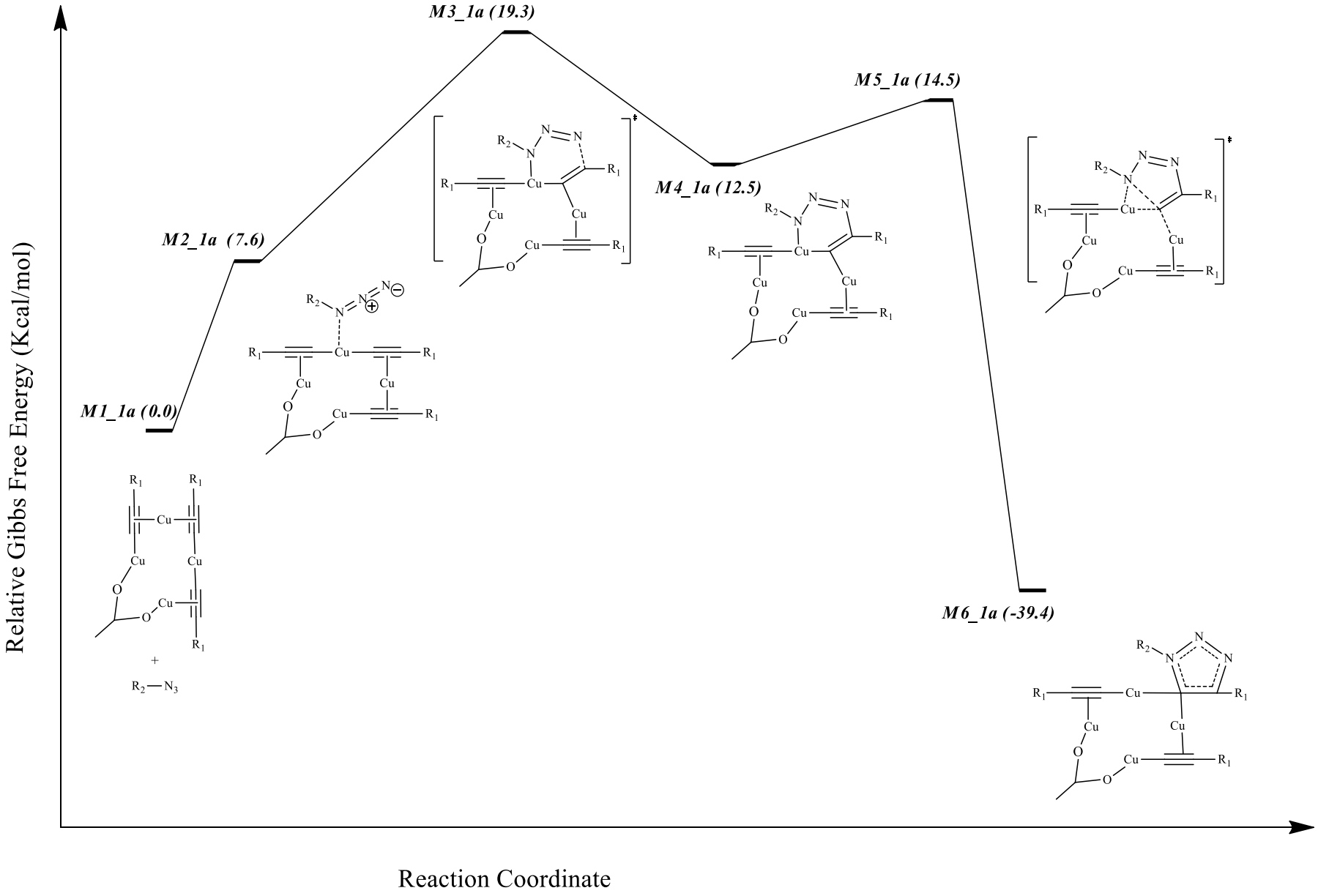

Figure 4.11 : Cycloaddition mechanism with the copper acetylide structure containing one acetate as the ligand. (Free energies (kcal/mol) are relative to **M1_1a**)

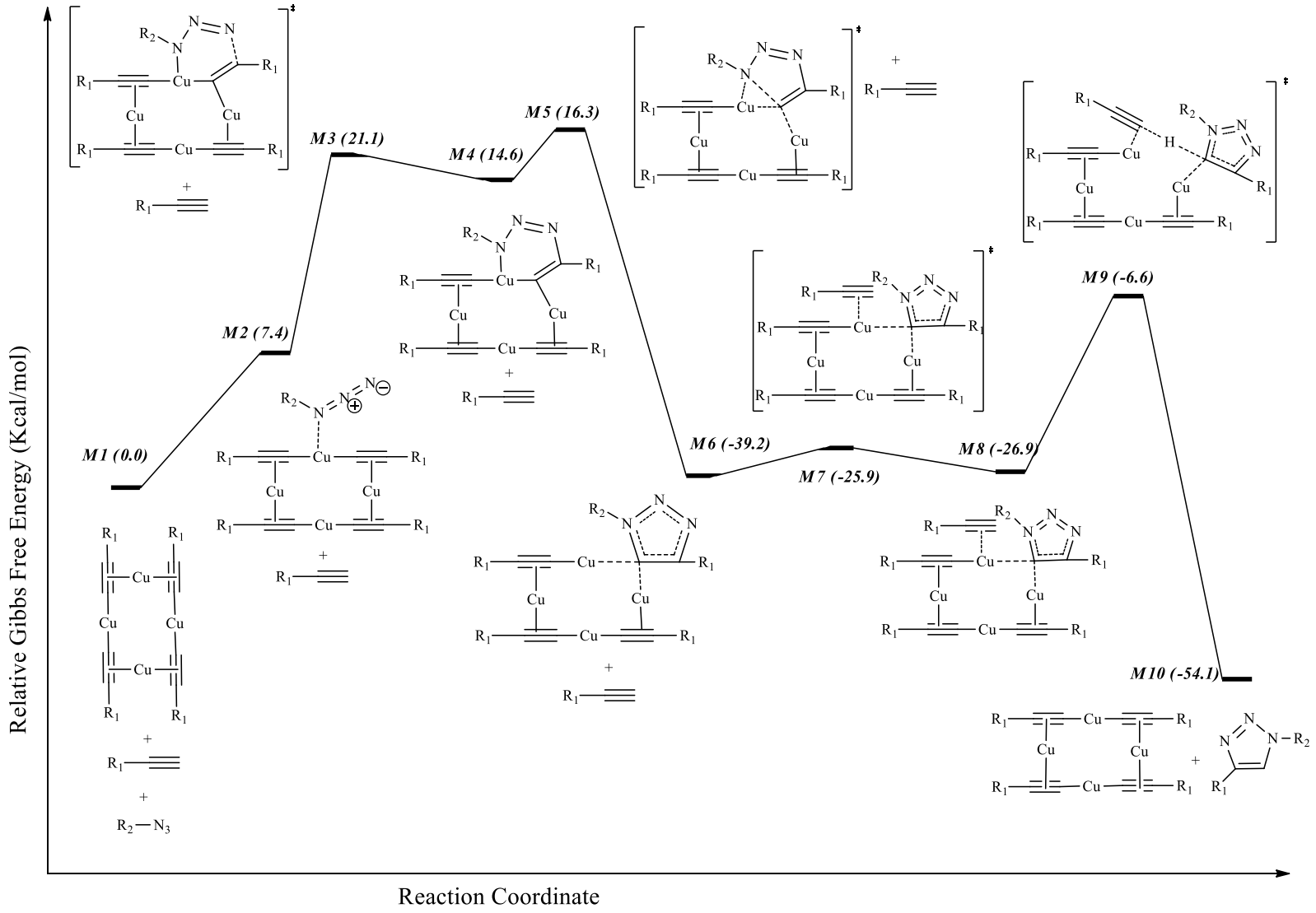

Figure 4.12 : Cycloaddition and protonation mechanisms in the absence of acetate as ligand and the alkyne as the H donor. (Free energies (in kcal/mol) are relative to **M1**[68]

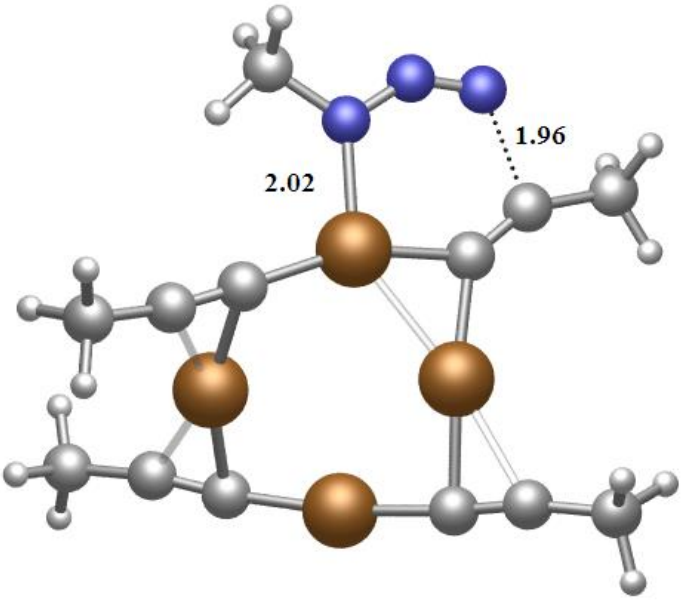

Figure 4.13 : Three-dimensional structure of **M3** transition state in cycloaddition mechanism in the presence of one acetate as the ligand [68].

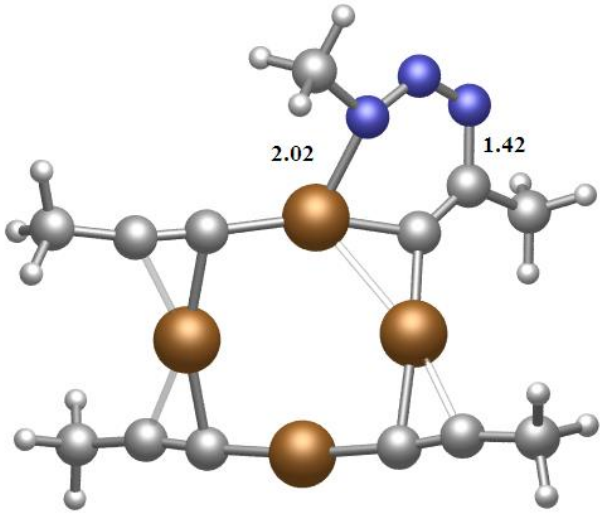

Figure 4.14 : Three-dimensional structure of **M5** transition state in cycloaddition mechanism in the presence of one acetate as the ligand [68].

4.1.2 Protonation

Once a copper-triazolide structure is formed, it is ready to undergo protonation which will free the triazole ring and also cause regeneration of the copper-acetylide structure. For modelling the protonation step two different proton donors, alkyne and acetic acid are used. The transition states and intermediates belonging to protonation from the alkyne will be referred with **-al** suffix and from the acetic acid with **-ac** suffix.

4.1.2.1 Alkyne as proton donor

After cycloaddition, alkyne will be approaching the system in order to deliver its acidic terminal. The first transition state structure of protonation path (**M7_1a_al,** Figure 4.15) is formation of an alkyne-copper complex between propyne and **M6_1a**. Barrier to complexation is 8.82 kcal/mol in terms of free energies. Complex formation reactions are generally exothermic reactions. In some cases, the entropic contribution enforces endergonic complexations. In the protonation case studies herein, the complex structure has a free energy slightly higher (0.50 kcal/mol) than the transition state structure (Figure 4.21). When electronic energies are compared, the situation is more complex. **M7_1a_al** transition state is 1.67 kcal/mol and **M8_1a_al** intermediate is 3.51 kcal/mol more stable than the initial **M6_1a** structure. In a previous analogous study, the same kind of complex formation between copper-acetylide and alkyne, complex was only 1.0 kcal/mol more stable (in terms of free energy) than the transition state (Figure 4.12). Further calculations are necessary to refine this finding: **M8_1a_al** structure should be checked for lower energy. Additionally, further calculations should be performed with other functionals to find out if this energy data is an artifact of methodology involved in calculations. Complex formations are driven by non-bonded interactions and these effects should be treated well in calculations. However, B3LYP is known to act poorly in van der waals structures, especially with non-covalent π interactions. M06-L functional can be a good alternative in this respect.

The electron-rich multiple bond of propyne interacts with copper, forming an interaction with Cu at 2.47 Å and 2.65 Å distances (Figure 4.15) in **M7_1a_al** which goes down to 2.06 Å and 2.14 Å in the **M8_1a_al** intermediate (Figure 4.16) due to

stronger binding of the alkyne. When geometries during the transition from **M6_1a** structure to **M7_1a _al** are analyzed, it is seen that the alkyne that is approaching propels the triazole group and maximizes the distance between 2 coppers to which the triazole group in **M6_1a** is linked to. This Cu-Cu distance was 2.49 Å in **M6_1a** and it rose to 2.54 Å in **M7_1a _al**. The Cu-$C_{triazole}$ bond also stretched to 2.25 Å in the **M8_1a_al** intermediate from 2.08 Å in its transition state structure.

After the formation of **M8_1a _al** intermediate, the alkyne group linked to Cu went through various geometric changes in order to provide H for the triazole ring. The olefinic carbon that will release its hydrogen to triazole reached the same plane. In the meantime, the bonding C--H distance which was 3.05 Å in **M8_1a_al** diminished to 1.43Å in **M9_1a_al** by elongation of the breaking C--H bond to 1.37 Å. In the course of all of these changes that would enable the H transfer from alkyne to triazole, no dramatic change occurred in the main skeleton. It was seen that after the triazole separated from copper structure, the deprotonated alkyne linked to the copper-acetylide and regenerated the **M1_1a** once again. In other words, starting from **M1_1a**, the CuAAC reaction cycle was completed and the reaction returned to its starting point as expected. This last deprotonation and detaching of triazole ring takes place via a barrier of 22.46 kcal/mol. Release of triazole ring is exergonic by 24.22 kcal/mol and the overall procedure of triazole formation is exergonic by 54.1 kcal/mol.

At this point, the presence of acetate group as ligand should be questioned in terms of energies and the structures on the reaction path. One clear difference is present in the **M7_1a _al** structure. In the presence of acetic acid, the approaching alkyne group does not bind to copper as strongly as it does in non-acetylated analog. The bonding Cu--C distances were 2.25 Å and 2.40 Å in **M7** (Figure 4.12). This transition is a late transition state as compared to its acetylated version and it is reflected in its higher barrier (13.3 kcal/mol *vs* 8.82 kcal/mol). Comparing the protonation steps shows no dramatic change in the barriers between the acetylated (Figure 4.21) and non-acetylated paths. The highest points on the reaction path are **M9** transition states and they are at almost the same relative energies. In the protonation mechanism, the main skeleton of coppers is conserved throughout the reaction. This indicates that the barrier to protonation is not affected by the acetyl group as ligand since the reaction site is in this case is away from the active part of the copper-complex and the main

skeleton of the copper-structure is not undergoing dramatic differences during the reaction.

4.1.2.2 Acetic acid as proton donor

Protonation is modelled with acetic acid as proton donor where acetic acid has contributed to the copper-acetylide structure as ligand. Unlike the case where alkyne is the donor, acetic acid deprotonation takes place in a single step (Figure 4.22). The initial acetic acid-copper complexation transition structure could not be found , mainly due to the acetic acid's ability to donate the H-atom. In the first transition structure, **M9_1a_ac**, while oxygen is transferring its labile H to the triazole ring at a distance of 1.49 Å, it simultaneously binds to copper. Once triazole ring forms, it detaches and forms a copper acetylide structure with two acetyl groups as ligands. The cycloaddition reaction can take place from the unreacted alkynes or ligand exchange can take place and reform the 4-copper centered copper-acetylide species. In previous studies performed by Özen et al. buky groups on alkynes have caused defragmentation of the copper-acetylide struture during the detachment of triazole ring. This was not considered vague since this reaction was reported to have a dynamic reaction order with respect to copper [40] and there still a debate on the number of copper atoms in the copper-acetylide structure. Calculations on two-copper species were shown to have almost the same reaction barrier. However, any deduction without actual calculations will be ambigous. Thus, in a reaction set with bulky groups, the presence of acetyl groups may lead to fragmentation as in previous case.

In the presence of acetic acid, with both ligand and donor, the highest point on the reaction path is -26.19 kcal/mol (Figure 4.22) whereas with alkyne as H-donor the reaction path is more steep (-7.62 kcal/mol, Figure 4.21). The energy values indicate that in the reaction medium, acetic acid will be the proton donor, which is also in accordance with basic chemical knowledge.

As the last part of protonation study, protonation from copper-triazolide structure via acetic acid is modelled (Figure 4.23). In this model, it is assumed that during cycloaddition acetic acid does not involve in copper-acetylide formation and is only involved in protonation and the release of triazole ring. In this model, from **M6** structure, acetic acid is acting to release its hydrogen to the triazole ring. As in Figure

4.22, a pre-reaction complex does not form and acetic acid directly transforms its H to the copper triazolide structure. The bonding and breaking bonds in this transition state is very much like **M9_1a_ac** transition state in Figure 4.19. In this transition state the distance between H and O of acetic acid is 1.20 Å ,Also The distance between $C_{triazole}$-H bond is 1.45 Å.The protonation barrier in this case is 18.6 kcal/mol. When compared with the data in Figure 4.22, it is seen that the presence of acetic acid as ligand facilitates protonation and takes place via a barrier of 13.21 kcal/mol. Likewise, comparison with protonation of **M6** from alkyne in Figure 4.12, the reaction is much more easily accomplished in the presence of acetic acid as H-donor.

The present protonation data shows that protonotion from copper-triazolide via alkyne requires high barriers whether acetate is present as ligand or not. When acetic acid is H-donor, the reaction is much more feasible, even easier with copper-triazolide containing acetyl group as ligand. Thus, proton donor is important in CuAAc reactions. The structure of copper-triazolide is not that important since the active part of the copper-triazolide is almost the same irrespective of the ligand bound to it.

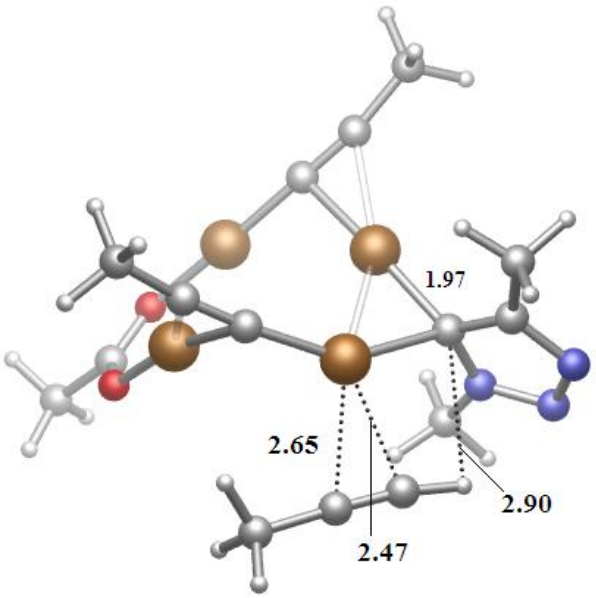

Figure 4.15 : Three-dimensional structure of **M7_1a_al** transition state in protonation mechanism in the presence of one acetate as the ligand .

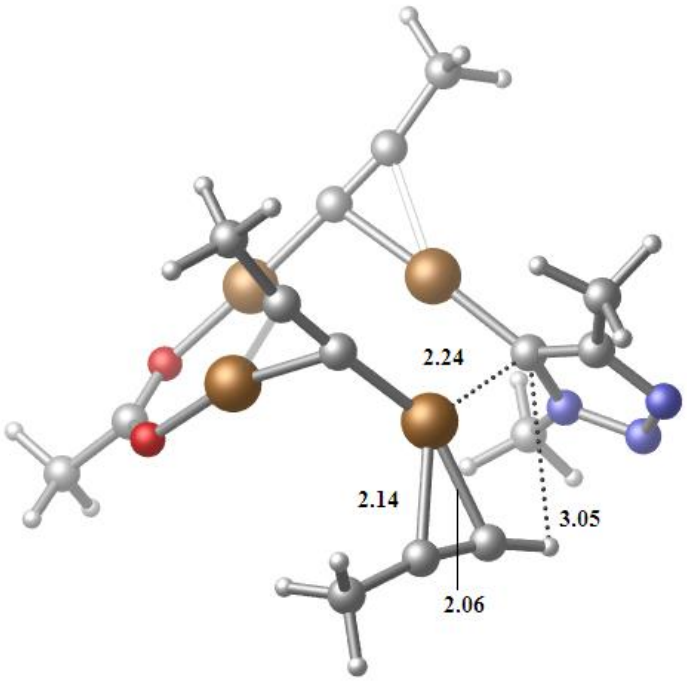

Figure 4.16 : Three-dimensional structure of **M8_1a_al** in protonation mechanism in the presence of one acetate as the ligand .

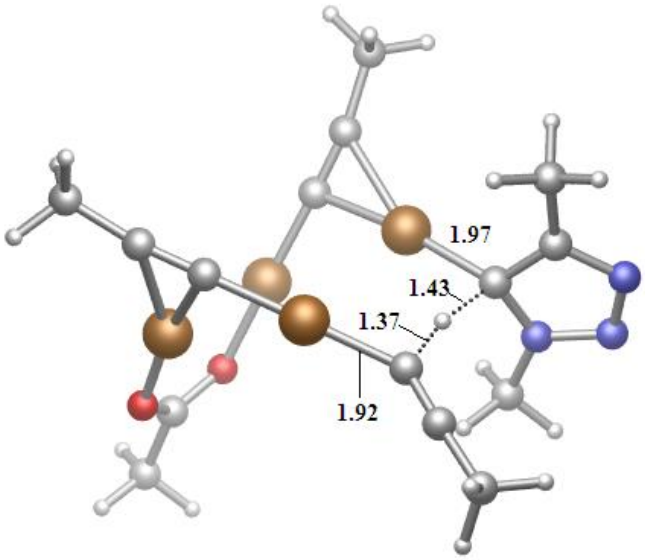

Figure 4.17 : Three-dimensional structure of **M9_1a_al** transition state in protonation mechanism in the presence of one acetate as the ligand .

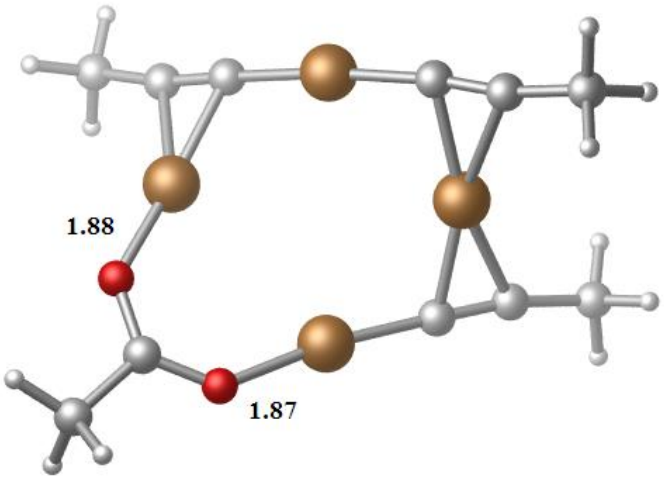

Figure 4.18 : Three-dimensional structure of **M10_1a_al** in protonation mechanism in the presence of one acetate as the ligand .

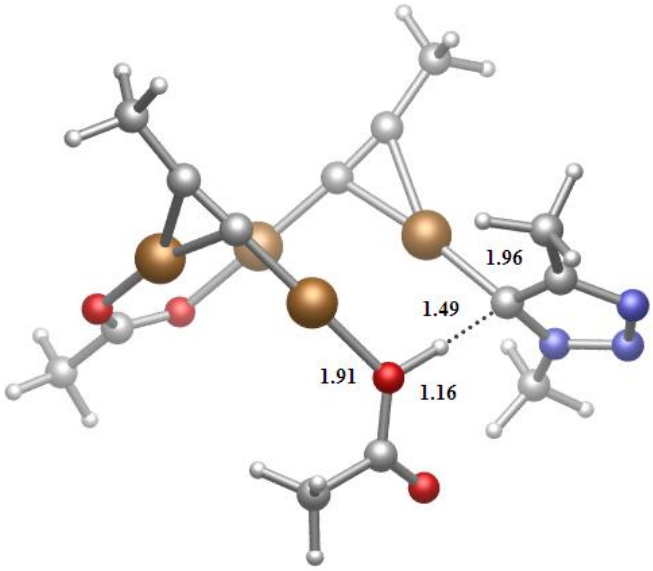

Figure 4.19 : Three-dimensional structure of **M9_1a_ac** transition state in protonation mechanism in the presence of one acetate as the ligand .

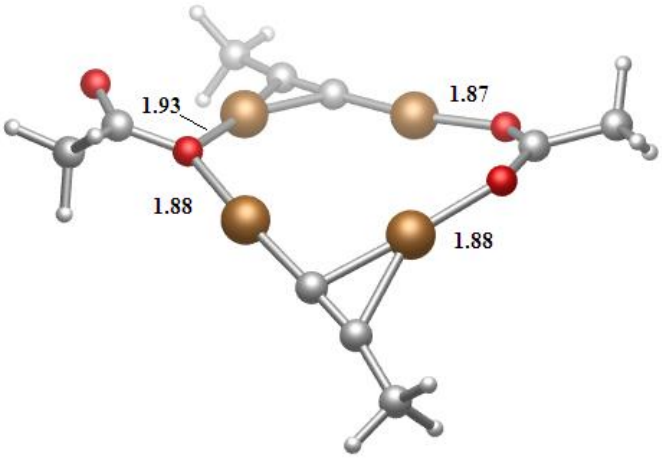

Figure 4.20 : Three-dimensional structure of **M10_1a_ac** in protonation mechanism in the presence of one acetate as the ligand .

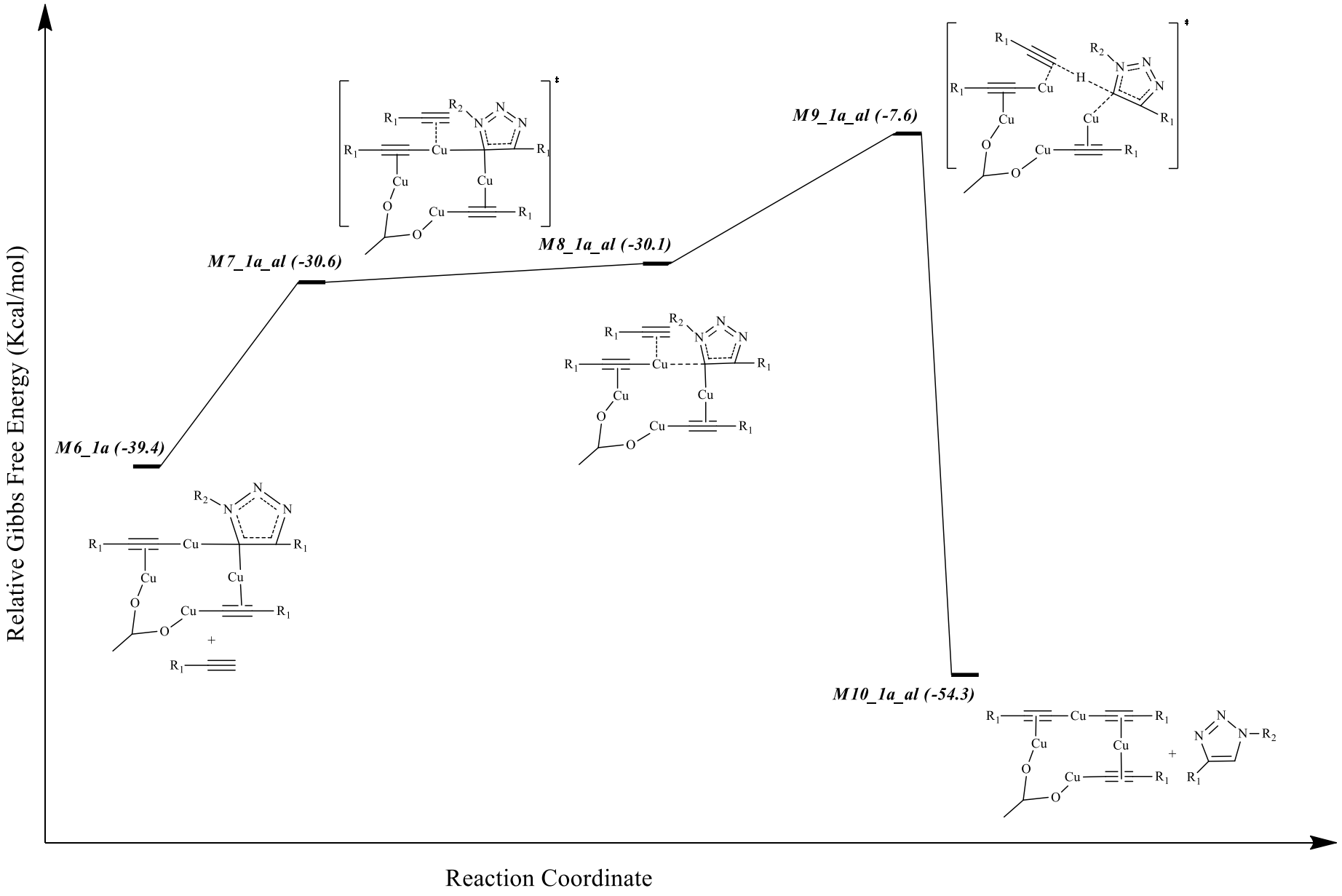

Figure 4.21 : Protonation mechanism of the copper-triazole structure containing one acetate as ligand via alkyne as proton donor. The Free energies (in kcal/mol) are relative energies as compared to copper-acetylide complex **M1_1a.**

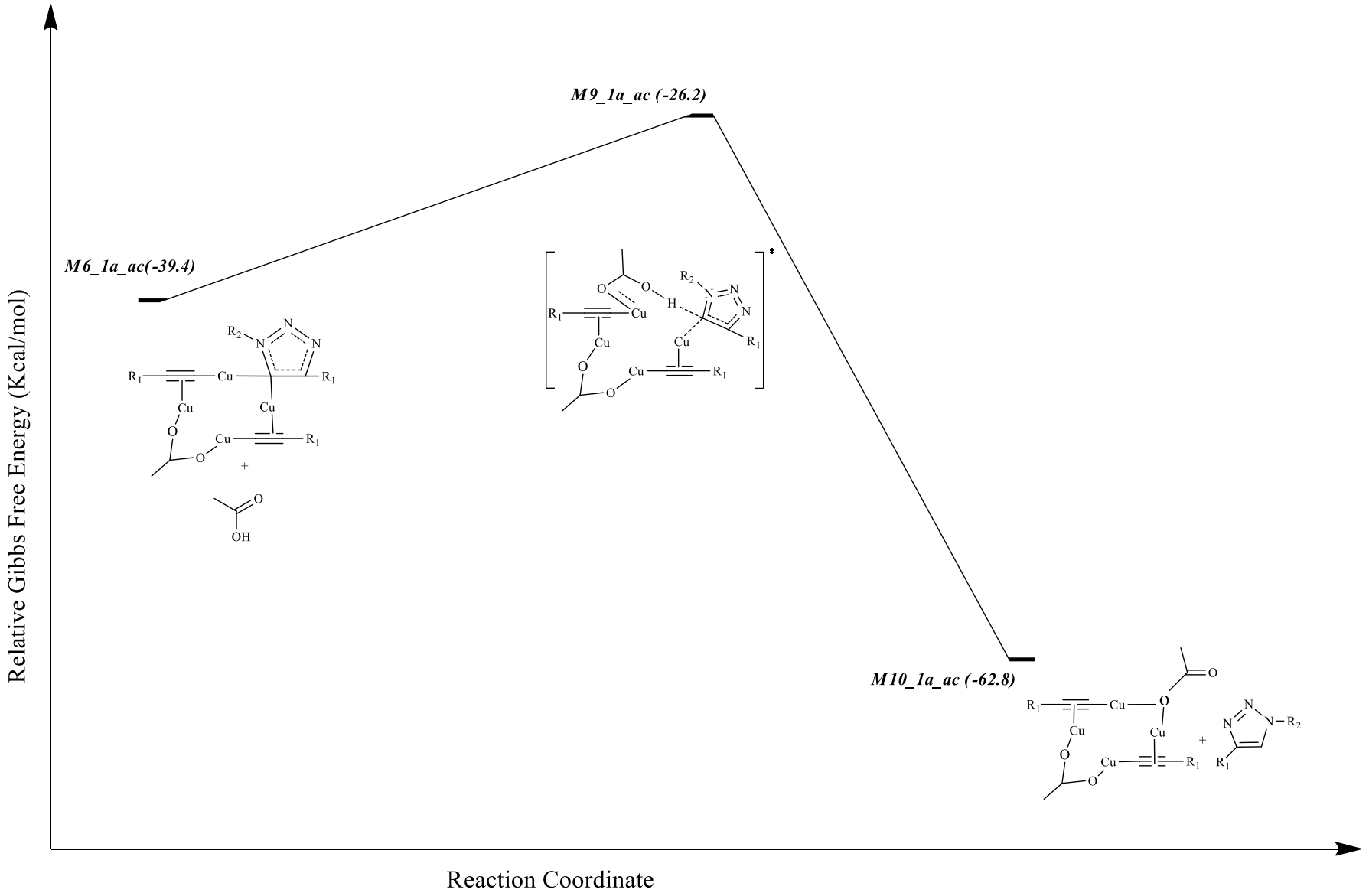

Figure 4.22 : Protonation mechanism of the copper-triazole structure containing one acetate as ligand via acetic acid as proton donor. The Free energies (in kcal/mol) are relative energies as compared to copper-acetylide complex **M1_1a**.

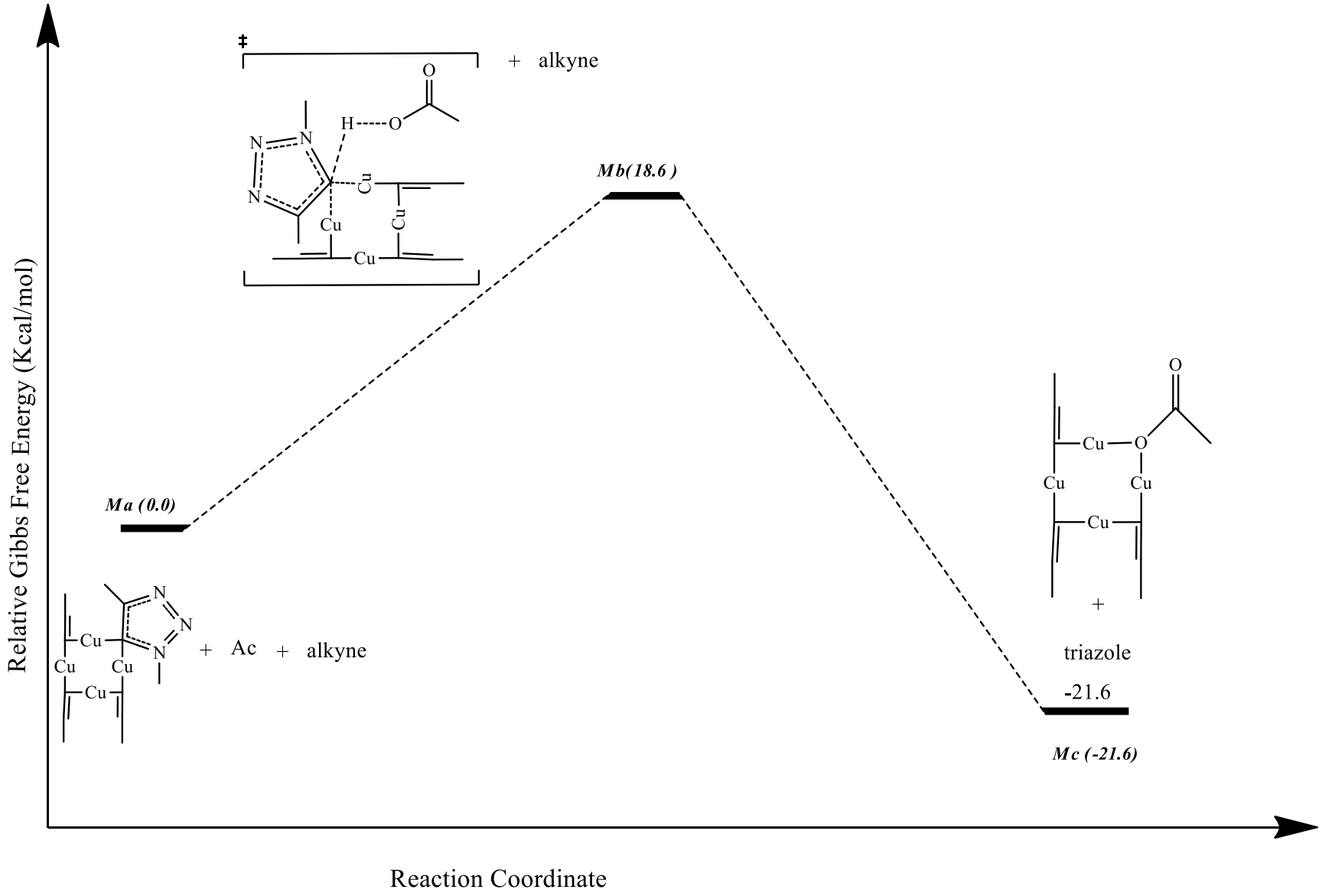

Figure 4.23 : Protonation mechanism from copper-triazolide in the absence of acetate as ligand but present as H donor. The Free energies (in kcal/mol) are relative energies as compared to copper-acetylide structure.

4.2 Modelling Copper-Acetylide Structures in CuAAC Reactions

To date, the CuAAC reaction mechanism has been the subject of numerous studies due to the significance of this reaction. However, the debate on the mechanism of CuAAC reaction has not finished.

The early studies performed indicated that CuAAC reaction mechanism takes place via one-copper metal in the copper-acetylide structure [32,37]. The kinetic studies carried out in recent years have suggested that the CuAAC reaction mechanism is 2^{nd} order with respect to copper and the reaction has multinuclear nature within the mechanism [40]. In addition to known data, the fact that the CuAAC reaction mechanism has multinuclear nature has been supported in a great number of theoretical and experimental studies [36,39]. Additionally, in a dissertation study carried out in our group, the starting copper-acetylide complex in CuAAC mechanism was modelled with 2,3 and 4- coppers [68]. In that study, 4-copper acetylide structures were proposed to form in the absence of ligands, based on their thermodynamic preferences and the tendency of copper to form polymeric copper-alkynes. Two-copper structures revealing the same reaction barrier as four-membered has indicated that the reaction can take place via 2-copper centered species. In a later study by Fokin *et al*.,an experimental study on CuAAC has been conducted [47]. In their study, 2 different copper isotopes have been used in order to illuminate the CuAAC reaction mechanism. From their work, they have suggested a mechanism functioning by means of two coppers (Figure 4.24-Figure 4.26). In this report, N-heterocyclic carbene (Figure 4.27-4.28) –ligated (NHC)copper acetylide structure with a natural isotopic ratio has been reacted with benzylazide in the presence of tetrakis(acetonitrile)copper(I) hexafluorophosphate with only a copper-63 isotope. At the end of the reaction, and as the result of the analysis of isolated copper triazolide structure, ^{63}Cu : ^{65}Cu ratio as 85:15 was changed through a 50 % enrichment. According to these results, Fokin pointed out that a ligand exchange had occurred in the course of the reaction and that the cause of the isotopic enrichment was the migration between NHC and MeCN [47].

In the light of all of this information, a mechanism was proposed via two copper-acetylide structures in the presence of ligans. In this dissertation study, the copper-acetylide complexes as suggested by Fokin et al have been modelled as a part of the continuing studies on CuAAC mechanism.

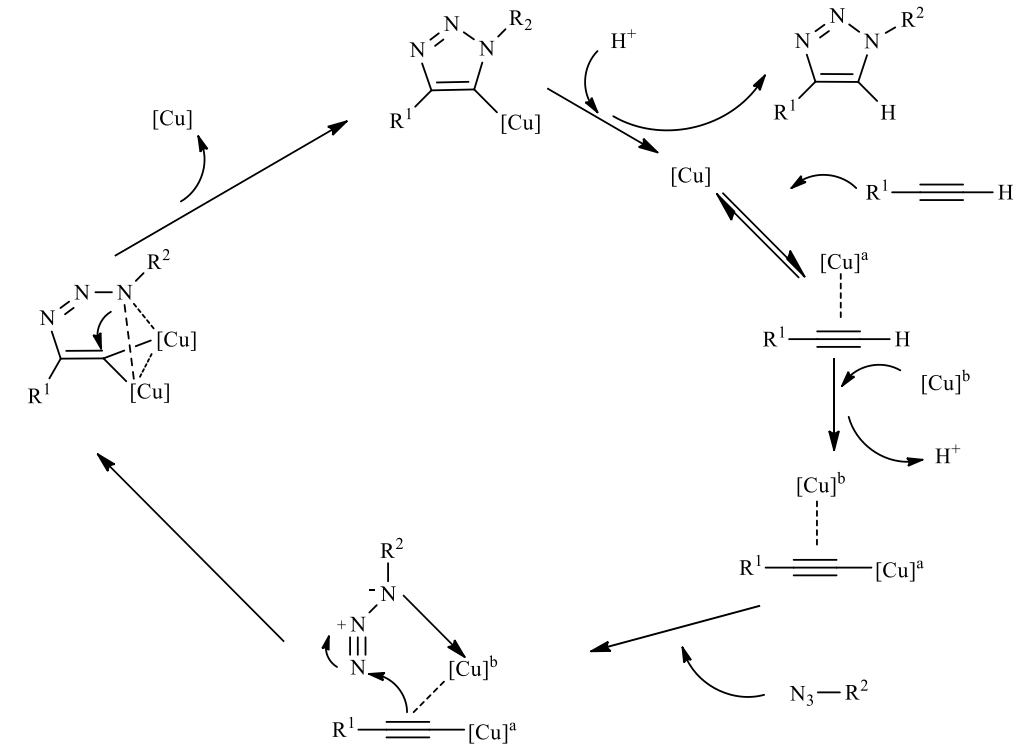

Figure 4.24 : General CuAAC mechanism proposed by Fokin et.al. [47].

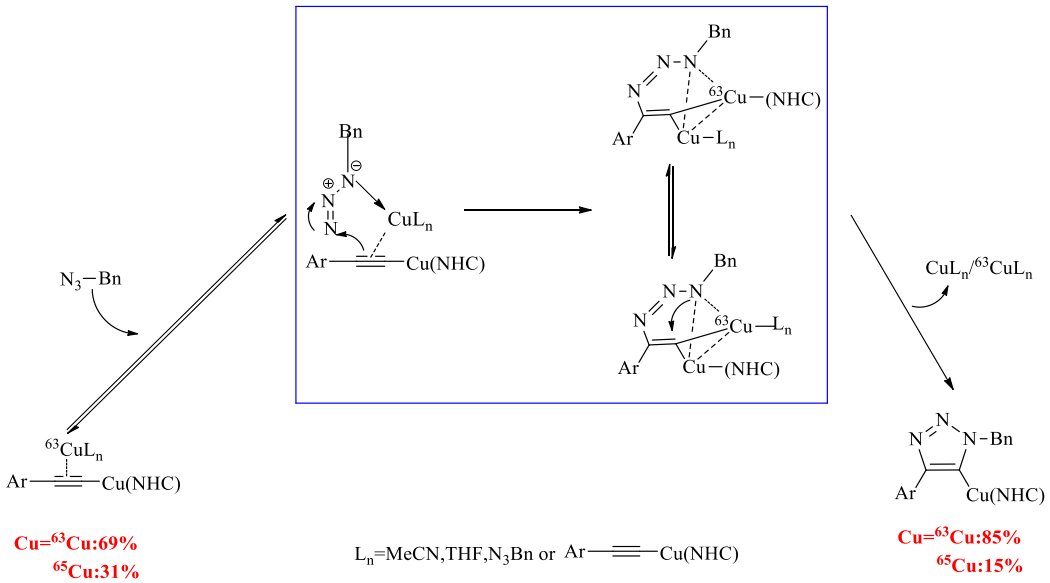

Figure 4.25 : Isotopic enrichment in mechanism proposed by Fokin *et.al.*[47].

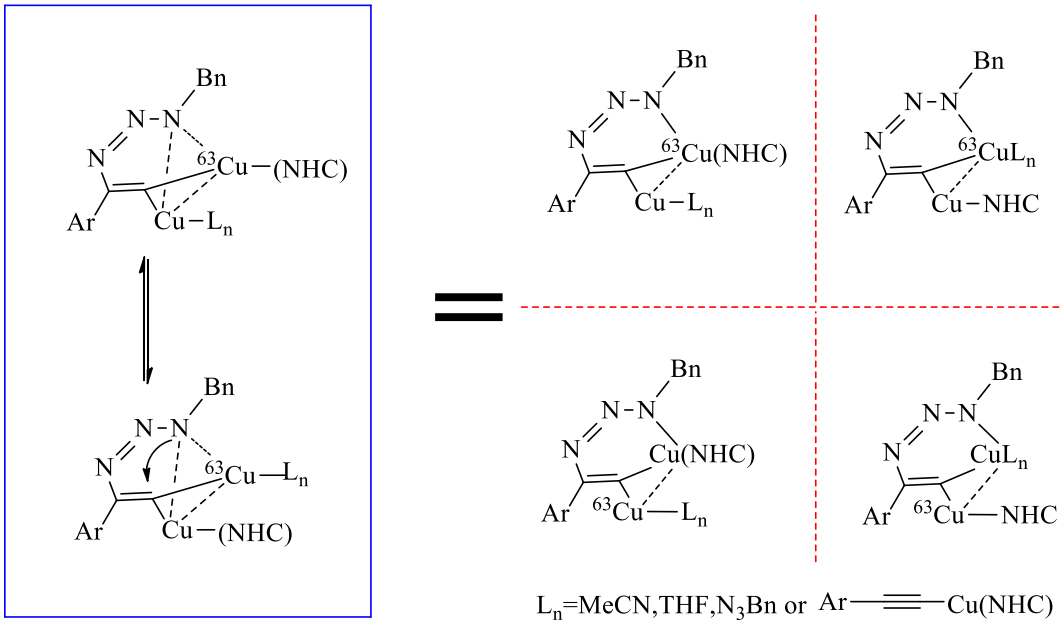

Figure 4.26 : Ligand exchange mechanism proposed by Fokin *et.al.* [47].

With the aim of testing the proposed mechanism, the initial NHC-ligated copper acetylide structure taking part in the proposed mechanism was modelled. In the experimentally proposed mechanism, the number of ligands were not determined. Thus, in the first place, two-copper species carrying one MeCN and NHC-ligated copper acetylide was modelled. In this structure, because of the number of electrons in the system, the species has to be either neutral doublet or cationic singlet. In the figures containing NHC ligand, due to the bulkiness of NHC, the actual 3-dimensional structures are not presented although it is included in the calculations. Instead green balls are used to indicate the position of the bulky groups on the ligand.

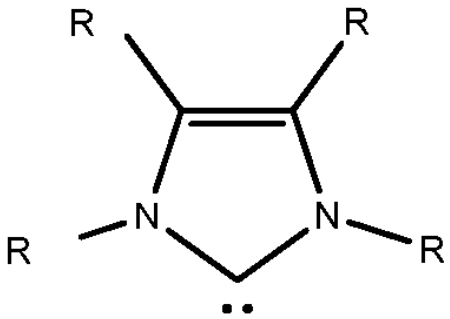

Figure 4.27 : Two-dimensional structure of NHC structure.

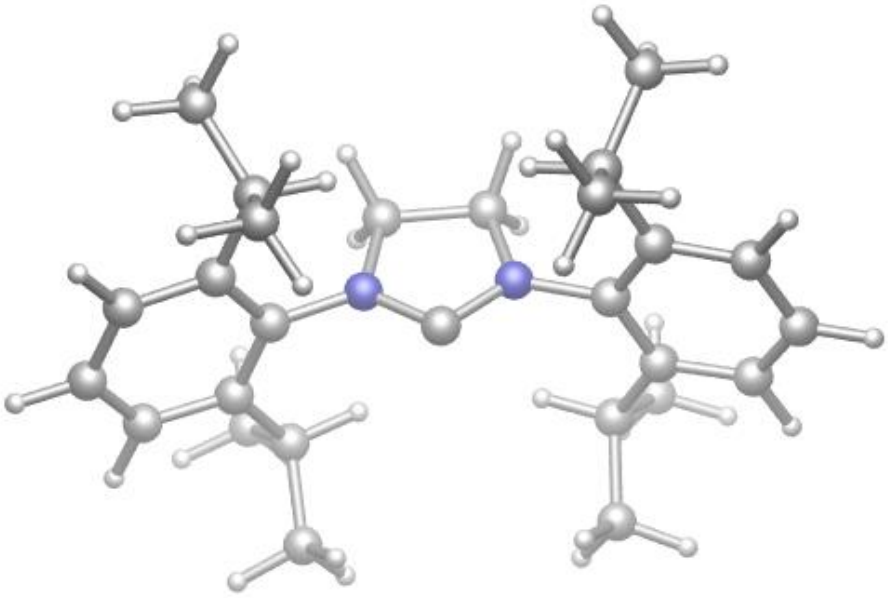

Figure 4.28 : Three-dimensional structure of NHC structure.

In the discussion that follows, the structures carrying 2 MeCN as ligand are designated as A and with one MeCN as B. In neutral doublet structures, the name of the structure has **+** or **d** the suffixes if the structure is singlet cationic or neutral doublet , respectively.

These studies were primarily made by using the B3LYP functional since the data to be obtained is desired to be compatible with the previous dataHowever, those structures were highly problematic in terms of geometry optimizations and convergence in terms of geometry or energy could hardly be obtained. On account of the problems encountered during the calculations, all the possible structures were tried to be re-modelled through the M06-L functional. This functional was suggested to perform well for transition metals. The obtained structures are presented in Figure 4.29-Figure 4.32). Further calculations of azide attack on the obtained A+, B+ and Bd structures were aimed to be performed however, no single structure could be obtained. These calculations are left as further study.

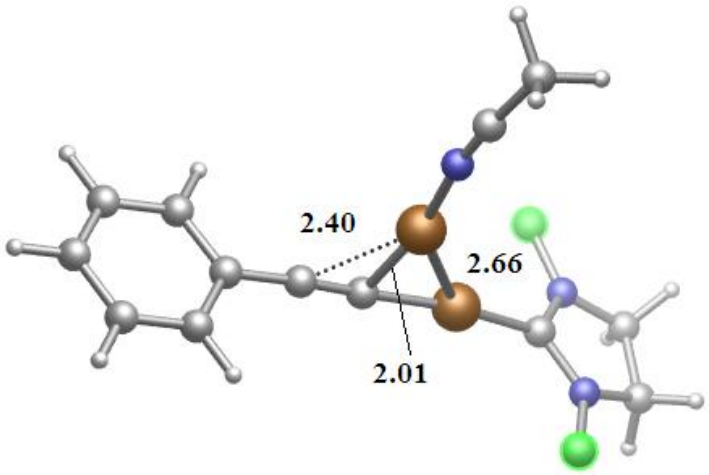

Figure 4.29 : Bd structure modeled with B3LYP functional.

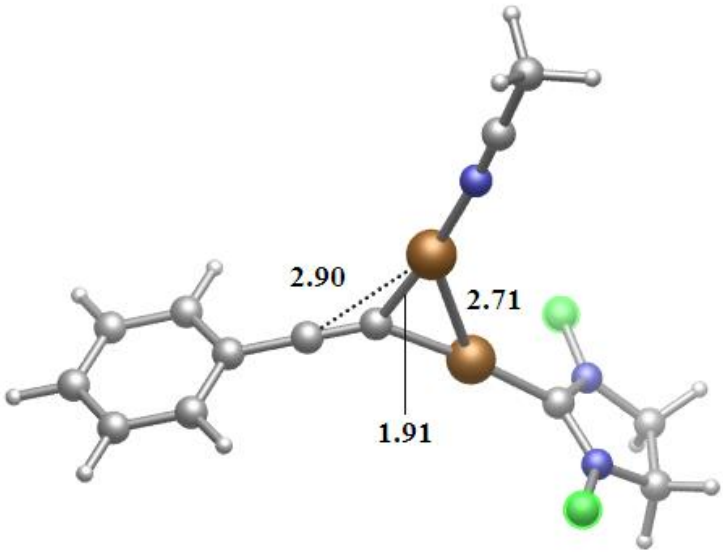

Figure 4.30 : B+ structure modeled with B3LYP functional.

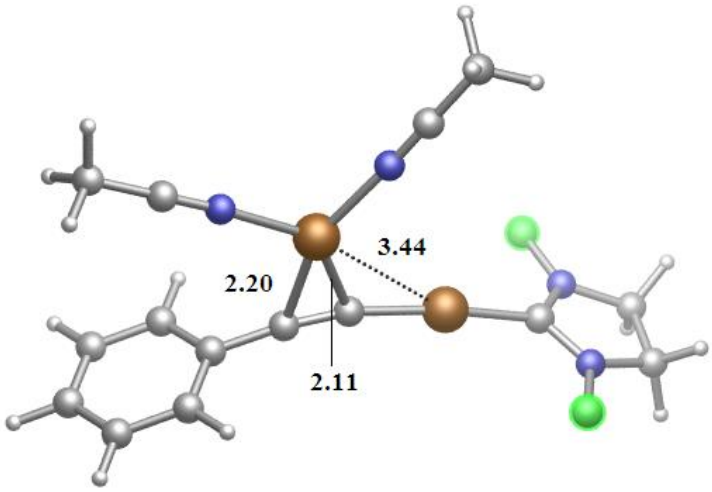

Figure 4.31 : A+ structure modeled with B3LYP functional.

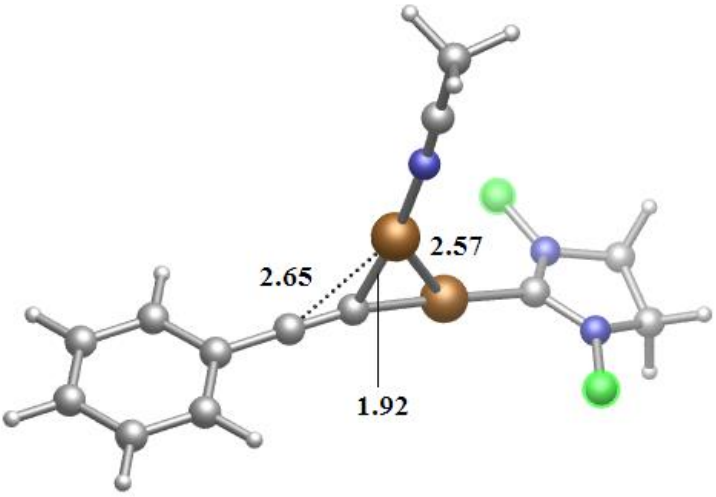

Figure 4.32 : B+ structure modeled with M06-L functional.

5. CONCLUSION

In this thesis, the copper-catalyzed azide-alkyne cycloaddition reaction (CuAAC), which was considered as a major break through in modern chemical synthesis methods, was studied with computational chemistry tools. Although the CuAAC methodology has been used in thousands of studies ranging from polymerizations to nanochemistry in the literature, the mechanims of the reaction has not been elucidated completely. As a part of ongoing projects on the mechanism of CuAAC, the cycloaddition and protonation steps of the reaction have been investigated in detail in this study. In the literature, it was pointed out by Straub et.al. [44] that the protonation step, which is the final stage of CuAAC reaction mechanism, would be faster in the presence of weak acid. Similar results were also reported by Hu, et. al.expressing that the protonation stage of CuAAC reaction taking place in an acidic environment enabled a serious increase in the reaction rate and shortened the reaction period. DFT calculations were first conducted whether the acetic has the possibility to act as ligand in the reaction. The calculations have shown that the presence of acetic acid as one ligand (**M1_1a**) is preferred thermodynamically as compared to all alkyne model (**M1**). The acetate group ligated cooper-acetylide structure was further used to model the cycloaddition reaction. In the presence of acetate as ligand, the generally proposed mechanism was shown to be a facile process. The geometries at the binding sites were found to be very similar with the previous study in which acetic acid was not considered. The comparison of cycloaddition barriers with and without acetic acid have not shown a significant change in the barriers. The presence of acetic acid decreases the relative energy by 1.80 kcal/mol at the highest point on the reaction path. This could accelerate the cycloaddition step. However, care must be taken at this point because in the **M1_1a** struture, there are 3 alkyne groups for the approaching azide to attack. In this thesis, only one of them, which was considered as the sterically least hindered one, has been considered. Considering one of the other two alkyne groups may further decrease the barrier. This has been left as a future work.

The protonation path serves as a regeneration path as well. In the protonation step two H-donor groups, alkyne and acetic acid and two copper-triazolide structures, the one containing acetate group as ligand and all alkyne analog have been considered.

In the presence of acetic acid, with both ligand and donor (Figure 4.22), the reaction is much more facile as compared to the case where alkyne is the H-donor (Figure 4.21). In the absence of acetic acid as ligand, protonation is again much more facile with acetic acid as H-donor (Figure 4.23) as compared to the alkyne (Figure 4.12). The energy values indicate that in the reaction medium, acetic acid will be the proton donor, which is also in accordance with basic chemical knowledge. More important data is the comparison of protonation paths starting from copper-triazolide structure with (Figure 4.21) or without (Figure 4.23) acetate group as ligand, where acetic acid is the proton donor. Among all the possibilities, the lowest barrier was observed for the case where acetic acid is acting both as ligand and as H-donor. Thus, it can be concluded that acetic acid is facilitating the reaction not only as an easy proton donor, but also acting as ligand and accelerating the reaction.

Cycloaddition reaction in the presence of acetate as ligand (Figure 4.11) decreases the barrier by approximately 2 kcal/mol. Without acetate ligand, considering the overal reaction, H abstraction step is highly energy requiring and can be the rate determining step of the reaction. However, in the presence of acetate both as ligand and donor, protonation is facile and cannot be rate determining step. Depending on the reaction conditions, protonation could be faster or slower. Based on this phenomenon Straub et al. has isolated a copper-triazolide species using a weak proton source and bulk substituents to retard protonation and concluded that the reaction rate is governed by the acidity of medium. Hu et al have reported similar results where facilitating an acidic environment has decreased the reaction times to a great extent. Additionally, protic solvents were reported to decrease the reaction times dramatically as compared to aprotic solvents. One of the reasons was attributed to the protonation step with protic solvents being relatively fast due to the facility of proton donors [4b]. In this respect, our results show that protonation step has a crucial role on the kinetics of the CuAAC reactions and they are in accordance with the experiments.

In the second part of the thesis, experimentally proposed copper acetylide structures were aimed to be modelled, however, the proposed structures could not be obtained

with the methodology employed in this study. As future work, structures can be modelled by other functional or basis sets, or the model structures can be modified.

The calculations in this study have been performed in vacuum, thus, solvent corrections are essential. In previous studies on cycloaddition and protonation, solvent calculations were found to have no significant effect on the barriers. Nevertheless, solvent calculations have to be performed as a check. Secondly, protonation has been considered only from one of the alkyne groups. Other alkynes should be tested as possible sites of cycloaddition. Although B3LYP functional is the most frequently used functional and successful in many cases, the results should be checked for the known deficiencies of this functional. M06-L calculations on the obtained paths are planned as future work.

6. REFERENCES

[1] **Tome, A.C.** (2004).Five-Membered Hetarenes with Three or More Heteroatoms In Science of Synthesis:Houben-Weyl Methods of Molecular Transformations,13,*(ed. R. C. Storr and T. L. Gilchrist*), Thieme, Stuttgart,415–601.

[2] **Krivopalov, V. P. and Shkurko, O. P**. (2005). 1,2,3-Triazole and its derivatives. Development of methods for the formation of the triazole ring, *Russian Chemical Reviews*, 74, 339–379.

[3] **Grana, G.** (2006). Adjuvant aromatase inhibitor therapy for early breast cancer: A review of the most recent data, *Journal of Surgical Oncology*, 7, 586-592.

[4] **Chao, S., Oh, S., Um, Y. Jung, J. H., Ham, J., Shin, W. S. and Lee, S.** (2009). Synthesis of 10-substituted triazolyl artemisinins possessing anticancer activity via Huisgen 1,3-dipolar cylcoaddition, *Bioorganic and Medicinal Chemistry Letters*, 19, 382-385.

[5] **Zhang, J.-J., Garrossian, M., Gardner, D., Garrossian, A., Chang, Y.-T., Kim, Y. K. and Tom Chang, C.** (2008). Synthesis and anticancer activity studies of cyclopamine derivatives, *Bioorganic and Medicinal Chemistry Letters*, 18, 1359-1363.

[6**] Odlo, K., Hentzen, J., dit Chabert, J. F., Ducki, S., Gani, O. A. B. S. M., Sylte, I., Skerede, M., Flørenes, V. A. and Hansen, T. V.** (2008). 1,5-Disubstituted 1,2,3-triazoles as cis-restricted analogues of combretastatin A-4: Synthesis, molecular modeling and evaluation as cytotoxic agents and inhibitors of tubulin, *Bioorganic and Medicinal Chemistry*, 16, 4829-4838.

[7] **Genin, M. J., Allwine, D. A., Anderson, D. J., Barbachyn, M. R., Emmert, D. E., Garmon, S. A., Graber, D. R., Grega, K. C., Hester, J. B., Hutchinson, D. K., Morris, J., Reischer, R. J., Ford, C. W., Zurenko, G. E., Hamel, J. C., Schaadt, R. D., Stapert, D. and Yagi, B. H.** (2000). Substituent Effects on the Antibacterial Activity of Nitrogen−Carbon-Linked (Azolylphenyl)oxazolidinones with Expanded Activity Against the Fastidious Gram-Negative Organisms Haemophilus influenzae and Moraxella catarrhalis, *Journal of Medicinal Chemistry*, 43, 953-970.

[8] **Périon, R., Ferrières, V., García- Moreno, M. I., Mellet, C. O., Duval, R., Fernández, J. M. G. and Plusquellec, D.** (2005). 1,2,3-Triazoles and related glycoconjugates as new glycosidase inhibitors, *Tetrahedron*, 61, 9118-9128.

[9] **Kokil, R.G.** (2010). Synthesis and In Vitro Evaluation of Novel 1,2,4-Triazole Derivatives as Antifungal Agents, *Letters in drug Design & Discovery, 7*, 46-49.

[10] **Sztanke, K., Tuzimski, T., Rzymowska, J., Pasternak, K., Szerszen, M.K.** (2008). Synthesis, determination of the lipophilicity, anticancer and antimicrobial properties of some fused 1,2,4-triazole derivatives,*Eur. J. Med. Chem.*, 43, 404-419.

[11] **Buckle, D. R., Rockell, C. J. M., Smith, H. and Spicer, B. A.** (1986). Studies on 1,2,3-triazoles. 13. (Piperazinylalkoxy)-[1]benzopyrano[2,3-d]-1,2,3-triazol-9(1H)-ones with combined H1-antihistamine and mast cell stabilizing properties, *Journal of Medicinal Chemistry*, 29, 2262-2267.

[12] **Joan, C. F. T., Elizabeth, H., Beatrice, M. and Daniel, P. B.** (1998). In Vitro Activity of a New Oral Triazole, *Antimicrobial Agents and Chemotherapy*, 42, 313-318.

[13] **Upmanyu, N.** (2006). Triazoles: As A Promising Medicinal Agents, 4, 3.

[14] **Singh, H., Shukla, K.N., Dwivedi, R., Yadav, L.D.** (1990). Cycloaddition of 4-amino-3-mercapto-1,2,4-triazole to heterocumulenes and antifungal activity of the resulting 1,2,4-triazolo[3,4-c]-1,2-dithia-4,5-diazines, *J. Agric. Food Chem*, 38 (7), 1483-1486.

[15] **Ezabadi, R.I., Camoutsis, C., Zoumpoulakis, P., Geronikaki, A., Sokovic, M. and Glamocilija, A.** (2008). Sulfonamide-1,2,4-triazole derivatives as antifungal and antibacterial agents: Synthesis, biological evaluation, lipophilicity, and conformational studies, *Bioorg. Med Chem.*, 16, 1150–1161.

[16**] Guo, L., Li, Z., Wang, H. and Zhang, C. Ye, D.** (2006). Carboxyamido-triazole inhibits proliferation of human breast cancer cells via G2/M cell cycle arrest and apoptosis, *European Journal of Pharmacology*, 538, 15-22.

[17] **Demirbas, N.** (2004). Synthesis and antimicrobial activities of some new 1-(5-phenylamino-[1,3,4]thiadiazol-2-yl)methyl-5-oxo-[1,2,4]triazole and 1-(4-phenyl-5-thioxo-[1,2,4]triazol-3-yl)methyl-5oxo[1,2,4]triazolederivatives, *Eur. J of Med Chem.*,39,793–804.

[18] **Huisgen, R.** (1984). In 1,3-Dipolar Cycloadditional Chemistry, Ed.: A. Padwa, Wiley, New York.

[19] **Sung, K., Lee, A.R.** (1992). Synthesis of [(4,5-disubstituted-4*H*-1,2,4-triazol-3-yl)thio]alkanoic acids and their analogues as possible antiinflammatory agents, *J Heterocyclic Chem.,* 29, 1101-1109.

[20] **Prasad, A.R., Rao, A.N., Ramalingan, T. and Sattur, P.B**. (1988). Indian Drugs, 25(7), 301-304.

[21] **Kumar, H., Javed, A.S., Khan, A.S. and Amir, M.** (2008). 1,3,4-Oxadiazole/thiadiazole and 1,2,4-triazole derivatives of biphenyl-4-yloxy acetic acid: synthesis and preliminary evaluation of biological properties,*Eur J Med Chem*, 43, 2688-2698.

[22] **Mhasalkar, M.Y., Shah, M. H. ,Nikam, S.T. and Deliwda,C.V.** (1970). 4-Alkyl-5-aryl-4H-1,2,4-triazole-3-thiols as hypoglycemic agents,*J Med Chem.*, 13(4), 672-676.

[23] **Gothelf, K.V., and Jorgensen, K.A.** (1998). A review of asymmetric 1,3-dipolar cycloaddition reactions, *Chemical Reviews*, 98, 863-909.

[24] **Mulzer, J.** (1991). A review of synthetic applications organic synthesis highlights, 77–95.

[25] **Katritzky, A.R., and Singh, S.K.** (2002). Synthesis of C-Carbamoyl-1,2,3-triazoles by Microwave-Induced 1,3-Dipolar Cycloaddition of Organic Azides to Acetylenic Amides, *Journal of Organic Chemistry*, 67, 9077-9079.

[26] **Wang, Z.X., and Qin, H.L.** (2003) Regioselective synthesis of 1,2,3-triazole derivatives via 1,3-dipolar cycloaddition reactions in water, *Chemical Communications*, 2450-2451.

[27] **Harju, K., Vahermo, M., Mutikainen, I., and Yli-Kauhaluoma, J.** (2003) Solid-Phase Synthesis of 1,2,3-Triazoles via 1,3-Dipolar Cycloaddition, *Journal of Combinatorial Chemistry*, 5, 826-833.

[28] **Molteni, G., and Ponti, A.** (2003). Arylazide Cycloaddition to Methyl Propiolate: DFT-Based Quantitative Prediction of Regioselectivity, *Chemistry – A European Journal*, 9, 2770-2774.

[29] **Boren, B.C., Narayan, S., Rasmussen ,L. K., Zhang, L., Zhao, H., Lin, Z., Jia, G., and Fokin, V. V.** (2008). Ruthenium-Catalyzed Azide−Alkyne Cycloaddition: Scope and Mechanism, *Journal of American Chemical Society*, 130, 8923-8930.

[30] **Bastide, J.and Henri-Rousseau, O.** (1973). Bulletin de la Societe Chimique de France, 2294-2296.

[31] **Clarke, D., Mares, R. W., and McNab, H.** (1997). Preparation and pyrolysis of 1-(pyrazol-5-yl)-1,2,3-triazoles andrelated compounds, *Journal of the Chemical Society*, Perkin Transactions,1, 1799-1804.

[32] **Rostovtsev, V. V., Green, L. G., Fokin, V. V. and Sharpless, K. B.** (2002). A stepwise Huisgen cycloaddition process: Copper(I)-catalyzed regioselective "ligation" of azides and terminal alkynes, *Angew. Chem. Int. Ed.*, 41, 2596–2599.

[33] **Appukkuttan, P., Dehaen, W., Fokin, V. V., and van der Eycken, E.** (2004). A Microwave-Assisted Click Chemistry Synthesis of 1,4-Disubstituted 1,2,3-Triazoles via a Copper(I)-Catalyzed Three-Component Reaction, *Organic Letters*, 6, 4223-4225.

[34] **Hein J. E., and Fokin, V. V.** (2010).Copper-catalyzed azide–alkynecycloaddition (CuAAC) and beyond: new reactivity of copper(I) acetylides, *Chemical Society Reviews*, 39, 1302-1315.

[35] **Bock, V. D., Hiemstra, H., and. van Maarseveen, J. H.** (2006).Cu(I)-Catalyzed Alkyne–Azide "Click" Cycloadditions from a Mechanistic and Synthetic Perspective, *European Journal of Organic Chemistry*, 51-68.

[36] **Himo, F., Lovell, T., Hilgraf, R. V., Rostovtsev, V., Noodleman, L., Sharpless, K. B., and Fokin, V. V.** (2005). Copper(I)-catalyzed synthesis of azoles DFT study predicts unprecedented reactivity and intermediates, *Journal of American Chemical Society*, 127, 210–216.

[37] **Meldal, M. and Tornøe, C. W.** (2008). Cu-catalyzed azide-alkyne cycloaddition, *Chemical Reviews*, 108, 2952-3015.

[38] **Straub, B. F.** (2007).μ-Acetylide and μ-alkenylidene ligands in "click" triazole syntheses, *Chem. Commun*, 3868-3870.

[39] **Cantillo, D., Ávalos, M., Babiano, R., Cintas, P., Jiménez, J. L. and Palacios, J. C.** (2011). Assessing the whole range of CuAAC mechanisms by DFT calculations-on the intermediacy of copper acetylides, *Org. Biomol. Chem.*, 9, 2952-2958.

[40] **Rodionov, V. O., Fokin, V. V. and Finn, M. G.** (2005). Mechanism of the ligand-free Cu-I-catalyzed azide-alkyne cycloaddition reaction, *Angew. Chem. Int. Ed.*, 44, 2210-2215.

[41] **Ahlquist, M. and Fokin, V.V.** (2007). Enhanced Reactivity of Dinuclear Copper(I) Acetylides in Dipolar Cycloadditions , *Organometallics*, 26, 4389.

[42] **Calvo-Losada, S., Pino, M.S. and Quirante, J.J.** (2014). On the regioselectivity of the mononuclear copper-catalyzed cycloaddition of azide and alkynes (CuAAC). A quantum chemical topological study. , *J Mol Model.* , 20, 2187.

[43] **Tüzün, N.Ş. and Özen, C.** (2012). The mechanism of copper-catalyzed azide-alkyne cycloaddition reaction: a quantum mechanical investigation., *J. Mol. Graph. Model.*, 34, 101.

[44] **Nolte, C., Mayer, P. and Straub, B.F.** (2007). Isolation of a Copper(I) Triazolide: A "Click" Intermediate, *Angew. Chem.Int. Ed.*, 46, 2101.

[45] **Shao, C., Wang, X., Xu, J., Zhao, J., Zhang, Q. and Hu, Y.** (2010). Carboxylic Acid-Promoted Copper(I)-Catalyzed Azide-Alkyne Cycloaddition. , *J. Org. Chem.*, 75, 7002.

[46] **Shao, C., Zhu, R., Luo, S., Zhang, Q., Wang, X., Hu, Y.** (2011). Copper(I) oxide and benzoic acid 'on water': a highly practical and efficient catalytic system for copper(I)-catalyzed azide–alkyne cycloaddition., *Tetrahedron Letters*, 52, 3782.

[47] **Worrell ,B. T., Malik J. A., Fokin,V. V.** (2013). Direct Evidence of a Dinuclear Copper Intermediate in Cu(I)-Catalyzed Azide-Alkyne Cycloadditions, *Science*, 340, 457.

[48] **Atkins, P. and Friedman R.** (2005). Molecular Quantum Mechanics, Oxford University Press, Fourth Edition,287-289.

[49] **Hohenberg, P. and Kohn, W.** (1964). Inhomogeneous Electron Gas, *Physical Reviews*, 136, B864 - B871.

[50**] Hohenberg, P. and Kohn, W.** (1965). Self-Consistent Equations Including Exchange and Correlation Effects, *Physical Reviews*,140, A1133 - A1138.

[51] **Salahub, D. R. and Zerner, M. C.,** (1989). The Challenge of d and f Electrons, ACS, Washington, D.C..

[52] **Parr, R. G. and Yang, W.** (1989). Density-Functional Theory of Atoms and Molecules, Oxford Univ. Press, Oxford.

[53] **Roothan, C. C. J.** (1951) .New Developments in Molecular Orbital Theory, *Reviews of Modern Physics*, 23, 69 – 89.

[54] **Pople, J. A. and Nesbet, R. K.** (1954). Self-Consistent Orbitals for Radicals, *Journal of Chemical Physics*, 22, 571.

[55] **McWeeny, R. and Dierksen, G.** (1968). Self-Consistent Perturbation Theory II, *Journal of Chemical Physics*, 49, 4852-4856.

[56] **Becke, A.D.** (1993). Density-functional thermochemistry III The Role of Exact Exchange., *Journal of Chemical Physics*, 98, 5648-5652.

[57] **Jensen, F.** (1999). Introduction to Computational Chemistry, John Wiley and Sons, pp 150-350, England.

[58] **Gonzalez, C. and Schlegel, H.B.** (1989). An Improved Algorithm for Reaction Path Fallowing, *Journal of Chemical Physics*, 90, 2154.

[59] **Gonzalez, C. and Schlegel, H.B.** (1990). Reaction Path Following in mass-Weighted Internal Coordinates, *Journal of Physical Chemistry*, 94, 5523.

[60] Url-1<http://pac.iupac.org/publications/pac/pdf/1999/pdf/7110x1919.pdf> , accessed at 30.04.2014.

[61] **Pulay, P.**(1980). "Convergence acceleration of iterative sequences. the case of SCF iteration",*Chemical Physics Letters*,73 (2),393–398.

[62] **Pulay, P.**(1982). "Improved SCF Convergence Acceleration". *Journal of Computational Chemistry*, 3 (4),556–560.

[63] **Csaszar, P. and Pulay P.** (1984). Geometry optimization by direct inversion in the iterative subspace, *J. Mol. Struct.(THEOCHEM)*, 114, 31-34.

[64] **Farkas, Ö. and Schlegel, H.B.** (2002). Methods for optimizing large molecules Part III.-An improved algorithm for geometry optimization using direct inversion in the iterative subspace (GDIIS)-, *Phys. Chem. Chem. Phys*., 4, 11–15.

[65] **Frisch, M. J., Trucks, G. W., Schlegel, H. B., Scuseria, G. E., Robb, M. A., Cheeseman, J. R., Montgomery, J. A., Vreven, Jr., T., Kudin, K. N., Burant, J. C., Millam, J. M., Iyengar, S. S., Tomasi, J., Barone, V., Mennucci, B., Cossi, M., Scalmani, G., Rega, N., Petersson, G. A., Nakatsuji, H., Hada, M., Ehara, M., Toyota, K., Fukuda, R., Hasegawa, J., Ishida, M., Nakajima, T., Honda, Y., Kitao, O., Nakai, H., Klene, M., Li, X., Knox, J. E., Hratchian, H. P., Cross, J. B., Adamo, C., Jaramillo, Gomperts, R., Stratmann, R. E., Yazyev, O., Austin, A. J., Cammi, R., Pomelli, C., Ochterski, J. W., Ayala, P. Y, Morokuma, K., Voth, G. A., Salvador, P., Dannenberg, J. J., Zakrzewski, V. G., Dapprich, S., Daniels, A. D., Strain, M. C., Farkas, O., Malick, D. K., Rabuck, A. D., Raghavachari, K., Foresman, J. B., Ortiz, J. V., Cui, Baboul, A. G. , Clifford, S., Cioslowski, J., Stefanov, B. B., Liu, G., Liashenko, A., Piskorz, P., Komaromi, I.,RMartin, . L., Fox, D. J., Keith, T., Al-Laham, M. A., Peng, C. Y., Nanayakkara, A., Challacombe, M.,Gill, P. M. W., Johnson, B., Chen, W.,Wong, M.**

W., Gonzalez, C. and Pople J. A. (2004). Gaussian 03, Revision C.02, Gaussian, Inc., Wallingford CT.

[66] **Becke, A. D.**(1988) Density-Functional Exchange-Energy Approximation with Correct Asymptotic-Behavior. Phys. Rev. A 38, 3098–3100.

[67] **Zhao, Y. & Truhlar, D. G.**(2006) A New Local Density Functional for Main-Group Thermochemistry, Transition Metal Bonding, Thermochemical Kinetics, an Noncovalent Interactions. J. Chem. Phys. 125, 194101.

[68] **Ozen,C.**(2012). A Theoretical approach to The Mechanism of Copper-Catalyzed Furofuran and 1,2,3-Triazole Syntheses,ITU,Istanbul.

7. CURRICULUM VITAE

Candidate's full name:

Gamze KARAGAÇTI

Place and date of birth:

01.08.1987 - Keşan

Permanent Address:

Acıbadem mah. Meltem apt. 10/4 Üsküdar/İstanbul

Universities and Colleges attended:

ISTANBUL TECHNICAL UNIVERSITY (MASTER OF SCIENCE) CHEMISTRY	2011 - 2014
MARMARA UNIVERSITY (FACULTY OF EDUCATİONAL SCIENCE) CHEMISTRY TEACHER	2005 - 2010

Work Experience:

INCI ENERJI SALES AND MARKETING REPRESENTATIVE	2013-2013
ONKO KOCSEL MEDICAL REPRESENTATIVE	2012-2013